Tissue Engineering Intelligence unit 7
The Artificial Lung
Edited by Stiven N. Vaslef and Robert W. Anderson
Eurekah.com, Georgetown, Texas, 2002

CHAPTER 6

Gas Exchange in the Venous System: Support for the Failing Lung

Brack G. Hattler and William J. Federspiel

Introduction

Acute respiratory failure from a variety of causes is one of the main concerns in the care of patients in intensive care units. One form of severe, acute respiratory failure, the acute respiratory distress syndrome (ARDS), although first described by Ashbaugh in 1967, continues to exhibit a mortality rate of approximately 40-50% in spite of a better understanding of the pathophysiology responsible for this condition.[1,2] For the patient with acute respiratory failure, maintaining gas exchange at a level consistent with survival is associated frequently with progressively increasing levels of ventilator support. A review of our recent (1998) experience, with 1,839 patients who were placed on ventilators at the University of Pittsburgh, has indicated not surprisingly that mortality following intubation, oxygen delivery, and use of the respirator increases the longer the patient is ventilated (Fig. 6.1). Although a variety of diagnoses were responsible for initiating ventilator therapy, respiratory failure was listed as the primary cause of death in approximately 30% of patients. How use of the ventilator may contribute in a secondary manner to mortality is difficult to quantitate but may be more significant than has been appreciated and is addressed subsequently in this chapter. For the 799 patients within this group requiring ventilation for over 96 hours, a mortality of 37% was noted. These numbers are not unlike those found in other medical centers. The inability to accurately predict which patients will live and which patients will die from multiple organ failure and sepsis, versus those whose respiratory failure will contribute primarily to death, has led to an aggressive approach to respiratory support in this entire patient population. This approach is also based on the fact that mortality is the same regardless of whether the patient is classified as having simply acute lung failure or the more severe acute respiratory distress syndrome.[2-5] Of the 600,000 people in the United States who undergo ventilator therapy on an annual basis, approximately 240,000 patients require ventilation for 96 hours or more.[6,7] Costs to families, hospitals, and insurance carriers continue to escalate. Combined data for 90 medical centers in the United States for the year 1996 indicate a total cost of $3.8 billion with a mean mortality of 30.2% in patients on ventilators for 96 hours or greater at these institutions (Table 6.1).[8] Taking these circumscribed numbers and expanding them on a national scale indicate that intensive care costs for patients on a ventilator reflect a disproportionately large amount of the health care dollar. Any new therapies that can reduce the need for or intensity of ventilator support, including earlier weaning from mechanical

The Artificial Lung, edited by Steven N. Vaslef and Robert W. Anderson.

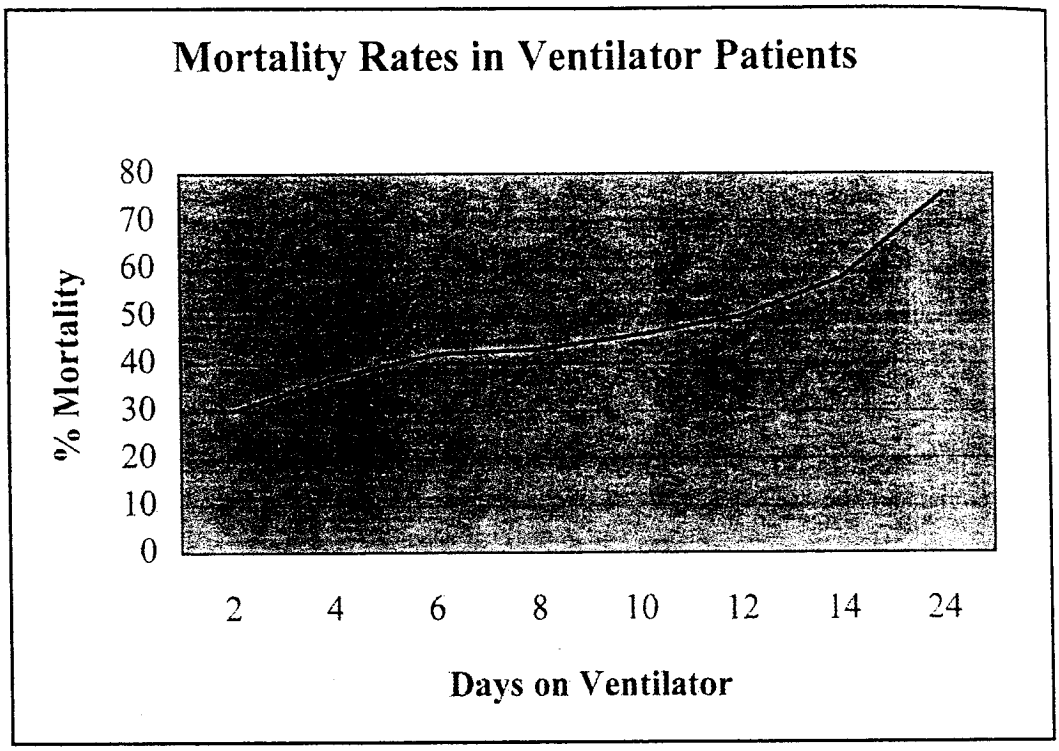

Fig. 6.1. Beginning at 48 hours after being placed on a respirator, a progressively increasing mortality is noted for the 1839 patients evaluated in the year 1998.

ventilation, should result in significant benefits in terms of patient suffering, patient ICU days, resource utilization, and earlier hospital discharge. These findings underscore the need for improved approaches to this patient population and constitute the basis for the continuing interest in the development of better ventilator strategies, new drug therapies, and artificial lung devices in the treatment of acute lung failure and in the management of patients on ventilators.[9-15]

This chapter describes progress in one of these areas as it relates to our development of an intravascular hollow fiber membrane lung assist device, the Hattler Respiratory Support Catheter or Hattler Catheter (HC) * that began with early prototype design and animal testing in 1984. These initial efforts were primitive compared to devices now being tested and involved bulky bundles of hollow fibers through which 100% oxygen would flow (Fig. 6.2). Both ends of each hollow fiber were potted into a single proximal manifold so that O_2 and CO_2 exchange would occur as the oxygen traversed the full length of the fiber. Kinking of the fibers at their distal tip was prevented by a wire loop. To avoid gas emboli, oxygen was vacuumed through the fibers. In vivo testing of these devices following surgical placement in the vena cava of dogs revealed that O_2 and CO_2 exchange occurred, but at levels (8-12 ml/minute) that were considered not to be of clinical value. It became apparent during these early experiments that passive flow of blood in the vena

* Also reported in previous publications as the Intravenous Membrane Oxygenator (IMO) for use in intracorporeal membrane oxygenation (ICMO). The catheter based device, however, exchanges both oxygen and carbon dioxide. Simply describing it as a membrane oxygenator is not sufficient. It is intended for respiratory support in cases of acute respiratory failure.

Table 6.1. Mortality, charges, and length of stay for patients from 90 medical centers on continuous mechanical ventilation for greater than 96 hours [1]

	Length of Stay (days)	Charges ($)	Patients (N)	Mortality (%)
Total		3,831,379,805	26,809	
Mean	34.0	61,796,448	426	30.2
Standard Deviation	5.9	44,612,280	178	6.4

[1]Data compiled for the year 1996 from University Health System Consortium; UHC Services Corporation; Oak Brook, IL.

cava, flow that was largely parallel to the hollow fibers, did not provide adequate gas exchange with these early prototypes. With this understanding, our efforts have evolved over the last 16 years with continued experimental work defining conditions that allow for improved gas exchange in the venous system.[16-21] We have emphasized our own experience having previously reviewed the contributions of others, beginning with the first published report by JD Mortensen in 1987 detailing his work in the development of the IVOX (intravenous oxygenator).[15, 22] The underlying concepts that are fundamental to gas exchange in blood have been instrumental in guiding research in this new field and have formed the basis for our approach in the development of the Hattler Catheter (HC), which stresses the science of bio-engineering as it applies to oxygen and carbon dioxide exchange in the venous system.

Background

Patients who are placed on ventilators for over 24 to 48 hours have, by definition, some form of acute respiratory failure that may occur in a setting of a de novo pulmonary disorder (i.e., pneumonia) or against a background of chronic lung disease. A prime example of the latter would be patients with chronic obstructive pulmonary disease (COPD) who develop an exacerbation of airflow obstruction with acute CO_2 retention (hypercapnic respiratory failure). The goals of mechanical ventilation in these two examples would be different with return of the lungs to their normal state in the case of the patient with pneumonia and support of the patient with COPD through the acute respiratory failure episode until he can be returned to his stable, chronically impaired pulmonary state. Modalities chosen for mechanical ventilation might vary depending upon whether the clinical presentation involved primarily hypoxemia or hypercapnia. The goal of mechanical ventilation, however, would be the same regardless of the patient on the respirator — that being reversal of the acute pulmonary process under conditions most favorable for healing of the lungs. In spite of this understanding, what has become only gradually apparent — initially through the early work of Kolobow and Gattinoni — is that iatrogenic injury caused by mechanical ventilation contributes to the morbidity and mortality of many ventilated patients.[23] Further contributions over the past 20 years by other scientists in the field have culminated in the recent publication of a trial sponsored by the National Institutes of Health, demonstrating an improved survival for patients on ventilators suffering from acute respiratory failure.[9] Patients were randomized to either "small breaths" (6 ml/

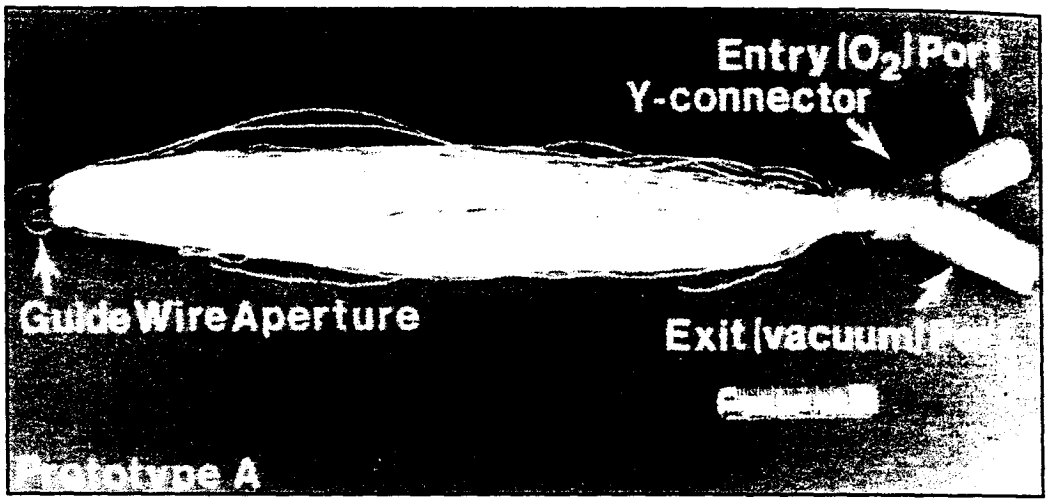

Fig. 6.2. Device manufactured and tested in dogs in 1984. See text for details.

kg tidal volume) or "large breaths" (12 ml/kg tidal volume) with all other respiratory parameters remaining the same. A 22% improvement in mortality was noted in the "small breath" group when compared with the "large breath" group (31% vs. 40% respectively). Permissive hypercapnia was seen in the "small breath" group. Some of these critically ill patients could not tolerate the reduced ventilation because of the increased P_{CO_2} levels. Respiratory acidosis with the use of lower tidal volumes has been noted by others.[24,25] A P_{CO_2} level greater than 70 mm Hg from a norm of 35-40 mm Hg can lead to an acute respiratory acidosis that is predominantly within the cell, potentially threatening cellular integrity. As tidal volumes fall, so does alveolar ventilation with a concomitant increase in the physiologic dead space. Bicarbonate administration and an increase in the respiratory rate do not fully correct for the progressive rise in P_{CO_2} which can reach dangerously high levels. Hypercapnia aggravates and worsens hypoxemia as CO_2 displaces O_2 at the alveolar level. The patient experiences various cardiorespiratory changes including an increased heart rate, an increased respiratory drive, and elevated pulmonary artery pressures.[26] Reducing the negative effects of acute hypercapnia would make reductions in tidal volume more universally feasible. In addition, the cellular effects of permissive hypercapnia may be partially compensated for by the improved hemodynamics associated with decreased tidal volumes and reduced airway pressures. The results of the NIH trial imply, therefore, that a further reduction in ventilation, in a setting where all patients would tolerate the therapy and the acute changes in P_{CO_2} levels would not occur, should lead to a consistent and even greater reduction in ventilator requirements and in mortality for patients in acute respiratory failure. This statement is strengthened by the fact that prior trials examining decreased tidal volumes, but not the very low tidal volumes per ideal body weight used in the NIH trial, did not demonstrate a difference between the treatment groups.[27-29]

It was not until the early 1960's, with the establishment of the first pulmonary intensive care units, that the pathology associated with respiratory barotrauma and pulmonary damage began to be clearly recognized, along with the role of oxygen in high concentrations as a toxic molecule often leading to progressive respiratory failure and death. Increasing concentrations of oxygen and delivered ventilator volumes and pressures produce in the patient and in experimental animals a noncardiogenic pulmonary edema. Histologically, damage occurs at the epithelial and endothelial cell level with mitochondrial swell-

ing, cytoplasmic disruptions, and nuclear degeneration. Platelet plugging and polymorphonuclear leukocyte (PMN) margination in the pulmonary capillary bed become increasingly prominent with gradual PMN spreading into the pulmonary parenchyma. Increased alveolar edema provides a setting for bacterial invasion, as does decreased ciliary action, tracheal-bronchial particle clearance, and surfactant inactivation.[30] Thus, the over zealous use of the very therapy intended for the treatment of acute respiratory failure can itself promote further lung damage and eventual death. A return to reduced inspired oxygen concentrations and ventilator settings before a lethal stage is reached can result in healing, survival, and, in later stages, avoidance of pulmonary fibrosis. Patients who survive severe forms of acute respiratory failure (i.e., ARDS) and its treatment frequently do well and resume normal levels of activity while others demonstrate progressive pulmonary fibrosis.[30] These findings have stressed the need for direct treatment strategies for acute lung failure that protects the lung not only from barotrauma and volutrauma but also from high partial pressures of oxygen.

A lung-protective strategy may have benefits in areas other than reducing direct injury to the lungs. Studies both in animals and in man have shown that over-distension of atelectatic lung segments, with their contained alveoli, elicits an inflammatory response marked by increased pulmonary and systemic cytokine concentrations.[31-33] Clinical studies support an association between elevated cytokine levels and an increased mortality in patients with acute respiratory failure on ventilators.[31] A recent randomized, controlled trial in patients with the acute respiratory distress syndrome has shown that mechanical ventilation can induce an elevated cytokine response (IL-6, TNF-α, IL-1β) in both broncho-alveolar lavage and plasma samples that is attenuated by a strategy to minimize overdistension and recruitment/derecruitment of the lung.[9, 32] Similar results have been noted in animal studies.[34] A correlation between elevated cytokine levels and multiple organ failure (MOF) has been reported.[31] It is difficult however, in the human, to differentiate between elevated cytokine levels because of multiple organ failure or multiple organ failure contributed to, and exacerbated by, a primary pulmonary source for cytokine production.[35,36] In the animal, however, these confounding variables are easier to control in a setting where the lungs begin in a normal state and are subjected to experimental manipulation while other organ systems are left relatively undisturbed. Here, time sequence-dependent variables can be discerned and indicate that mechanical ventilation can initiate an inflammatory response with ultimately systemic manifestations. These studies suggest that mechanical ventilation can contribute to the de novo development of multiple organ failure.[9, 31]

An equally important concern as it relates to multiple organ failure is the effect that mechanical ventilation has on the hemodynamic status and the microcirculation of these critically ill patients on respirators.[37] Ventilators and ventilatory maneuvers, especially in the setting of severe respiratory failure where part of the therapy involves vigorous diuresis and a lowered intravascular volume, can have profound effects on the heart and circulation. Positive end expiratory pressure (PEEP) levels (10 cm H_2O or greater) commonly employed in patients with acute respiratory failure lead to an increased intrathoracic pressure and a decrease in venous return with a concomitant drop in cardiac output and ejection efficiency. Increased pulmonary vascular resistance with an increased right ventricular afterload and a decrease in left ventricular compliance have also been reported under these circumstances. A primary concern surrounding changes in these parameters relates to what is happening with oxygen transport and oxygen content at the capillary level. Levels of PEEP of 10 cm of water have been reported to decrease oxygen transport in patients with

acute respiratory failure on ventilators.[38] The use of drugs to maintain the hemodynamic and cardiac status of the patient (i.e., epinephrine) becomes increasingly necessary and can lead to further vasoconstriction in the capillary beds, with a further decrease in tissue perfusion. A vicious cycle is, therefore, set in motion, where the end result is multiple organ failure and most frequently death. In Figure 6.3, the direct and indirect results of persistently high levels of mechanical ventilation are depicted. The patient on a ventilator, therefore, represents a highly complex set of physiological variables that are usually multi-factorial and reflect organ-system and patient-ventilation interactions. The ability to consistently and dramatically reduce ventilator support should reduce the incidence of death and its most frequent cause, multiple organ failure.

Other detrimental effects of prolonged intubation and mechanical ventilation are more difficult to quantitate and fall into the realm of hospital acquired pneumonias.[39] Prolonged intubation leads to airway microbial colonization and the risk of hospital acquired lower respiratory tract pneumonias. The risk of pneumonia increases the longer the patient is ventilated and mandates early extubation when clinically feasible. While pathological changes in the kidney, liver, and gastrointestinal tract can occur concomitantly with prolonged ventilator support, the most frequent and potentially lethal complications remain those of lower respiratory tract infections. A mortality greater than 10% has been reported with these ventilator associated pneumonias which lead to prolonged hospitalizations and greatly increased medical costs. The ability of the patient to be extubated, leave the intensive care unit, survive, and be discharged is significantly dependent, therefore, on the severity and number of complications associated with mechanical ventilation and the length of time a patient is on a ventilator.

Extracorporeal membrane oxygenation (ECMO) arose out of this need to rest the lungs. Early experience with ECMO however, was disappointing and multi-center trials demonstrated a 90% mortality in patients receiving joint ECMO and mechanical ventilation—no better than the group treated with mechanical ventilation alone.[40] For ECMO, an arteriovenous circuit was used at greater than 50% of cardiac output for blood flow to and from the externally positioned oxygenator, with an emphasis on oxygenation. A modification of ECMO, $ECCO_2R$, incorporated a veno-venous circuit with flows at 20 to 30% of the cardiac output, with an emphasis on CO_2 removal.[41] Veno-venous ECMO allows all blood that is removed and oxygenated to be returned to the patient via the venous-return cannula. This setting may provide a unique opportunity not present with veno-arterial ECMO for the injured lung to be favorably exposed to an increased level of oxygenated blood at the tissue level. Maintaining blood flow to the lungs would also favor metabolic and endocrine functions ascribed to these organs. Continued blood flow to the lungs and heart chambers as determined by the patient's cardiac output should also reduce any opportunity for thrombus formation within the vasculature of these organs. In the last 10 years, veno-venous access has been the support mode of choice at most major medical centers that are ECMO active. Intravenous gas exchange devices that are under development are essentially a simpler intravascular form of veno-venous ECMO and offer the same benefits. Both ECMO and $ECCO_2R$ have been included under the broader term extracorporeal life support (ECLS) and allow a reduction in ventilator settings, including ventilator frequency, ventilator volumes, and airway pressures. A combination of ECLS with a reduction in ventilator settings offers greater benefit than either therapy alone.[42-45] With these newer approaches to ECLS, expected survival has increased from 10% to 50% in adults with acute respiratory failure. Recent lessons learned in caring for patients with acute lung failure teach that the earlier ECMO is instituted, the greater the opportunity

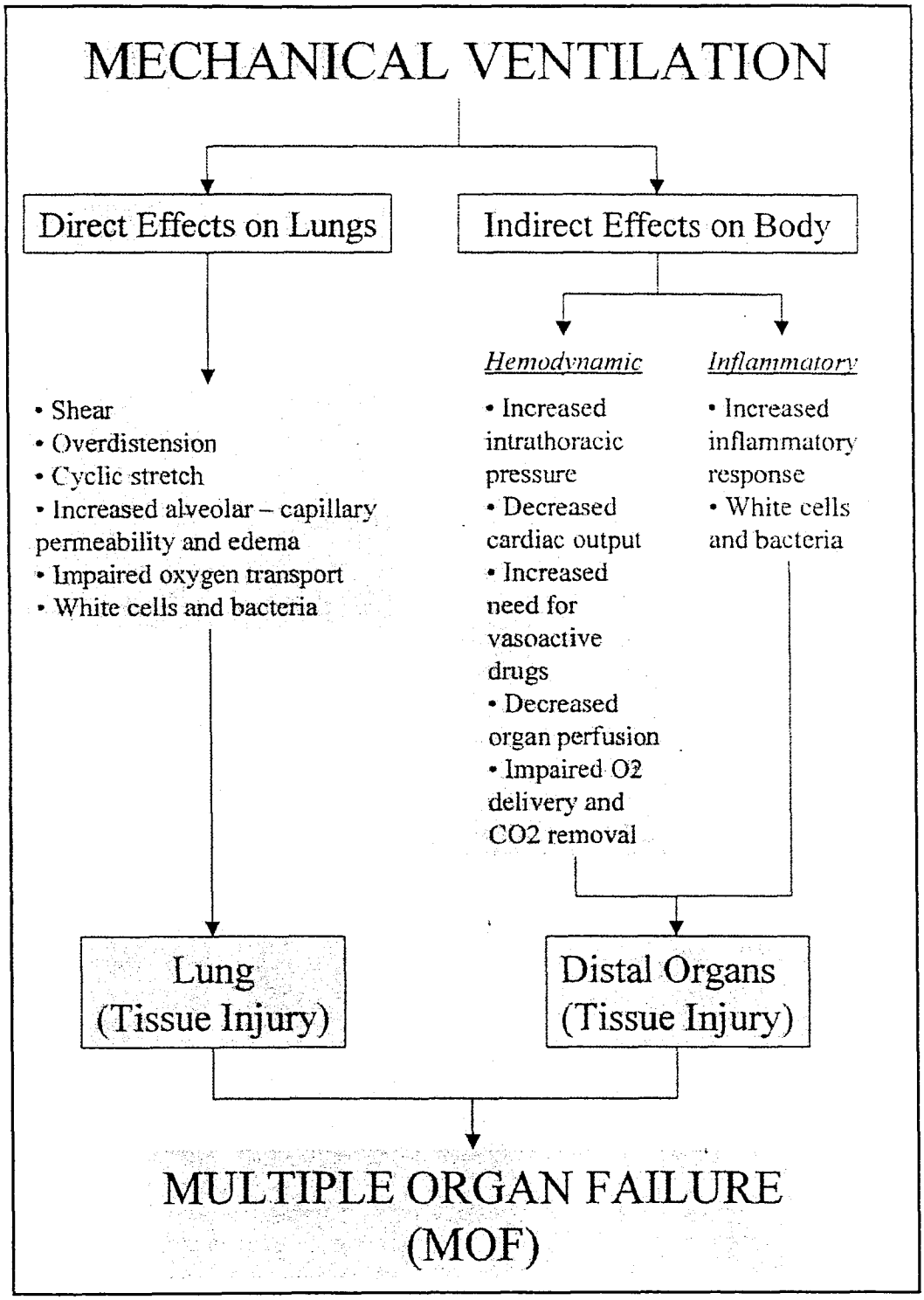

Fig 6.3. Direct and indirect detrimental effects of mechanical ventilation on patients. Adapted from references 31, 32, 33, 37.

for a successful outcome. Bartlett and his colleagues have reported that the number pre-ECLS days of mechanical ventilation is a significant predictor of outcome for survivors vs. nonsurvivors [2.7 days vs. 4.4 days respectively (P=0.0003)].[45] A similar approach to early intervention with lung failure before multiple organs become affected would be applicable to lung assist devices such as the Hattler Catheter. Extracorporeal life support, however, is a complex, personnel intensive, costly therapy that can only be carried out in the intensive care units of major medical centers where these resources are available and where complications from the therapy can be addressed. It does not serve, therefore, the majority of patients in community hospitals who are in need of a safer, relatively simple, inexpensive, and readily accepted therapy to treat patients with acute respiratory failure who are at risk for progressive lung injury while on the ventilator. Our approach to this dilemma has been to define new forms of therapy as they pertain to intravenous gas exchange that can benefit the patient with acute respiratory failure no matter whether he is admitted to a University or a community hospital. Here it has been important to note that even severe forms of respiratory failure are characterized by areas of both relatively normal and diseased tissues interspersed throughout the lungs.[46, 47] Intravenous devices currently under development are designed, therefore, to supplement without further injuring those areas of the lung that are functioning normally while diseased lung is allowed to heal. It is not anticipated at present that these devices will need to replace the entire lung function (mean resting exchange rates of 270 ml O_2/min and 240 ml CO_2/min). Based on the average percentage of the lung involved as seen on CT scans in the adult with ARDS and animal studies indicating the amount of residual lung required to meet basal requirements, the goal for the Hattler Catheter (HC) has been to provide at least 50% of basal O_2 consumption and CO_2 elimination (135 ml O_2/min; 120 ml CO_2/min).[46-48] This might appear difficult because of the anatomical constraints imposed by those sites where an intravenous device will affect gas exchange (i.e., inferior and superior vena cava and right atrium) without compromising hemodynamics. This limits the total hollow fiber membrane that can be introduced into the venous system to about 0.5 m^2 of fiber surface area. Certain conditions, however, can be created in a device that the natural lungs would not tolerate. The ability to maximize O_2 diffusion by introducing 100% oxygen at atmospheric pressure and to precisely control a rapid gas flow rate for CO_2 removal in hollow fiber membrane mats exposed to actively mixed blood over an extended blood path length has allowed us to reach a goal of 50% basal gas exchange rates and to establish certain basic principles as they apply in practice to the development of an intravenous membrane oxygenator.

Oxygenators have been available for over 40 years as external devices developed for gas exchange — O_2, CO_2, and other gases, including anesthetics — during extracorporeal circulation as it pertains to heart surgery. To minimize blood trauma and the incidence of gaseous and particulate emboli, hollow fiber membranes as the gas exchange component have replaced bubble oxygenators over the last 20 years in their use in the operating room. Although the oxygenator provides a gas exchange function similar to the natural lungs, the natural lungs function at a level that far exceeds the capability of any artificial lung and provide a total surface area for gas exchange that cannot be approached by present engineering solutions. The role of pulmonary support, however, is not to provide the extraordinary level of gas exchange achieved by the natural lungs. Rather, a gas exchange device, whether it be external as used in ECMO and open heart surgery, or internal, as used in an intravenous device, is intended to meet those gas exchange requirements necessary to maintain the patient's metabolic needs. For the patient during open-heart surgery, the oxygenator provides full gas exchange support during the cardiac procedure. For an

intravenous gas exchange device (the HC), only 50% of basal requirements can be met. It is therefore important to reemphasize that even in severe respiratory failure, injured tissue is interspersed with areas of normal lung, providing a setting where the patient can contribute to gas exchange through these functioning lung segments.[46, 47] Partial support with the intravenous device is therefore available as a supplement to the patient while normal lung segments are gently ventilated, and the damaged and diseased areas of lung are allowed to heal.

Clinical Trial of an Intravenous Respiratory Support Device

The only intravenous device for O_2 and CO_2 exchange that has undergone human clinical trials is the intravascular oxygenator (IVOX) developed by J. D. Mortensen.[22,49] The IVOX underwent human implantations in the early 1990's but was withdrawn from FDA consideration, partially because of the lack of concurrent controls and randomization in the trial, which failed to show improvement in survival compared with historical controls. The company that manufactured the IVOX is no longer operative. The device consists of a bundle of microporous hollow fiber membranes which are joined at the distal end of the device to the inner lumen of a double-lumen gas conduit and at the proximal end to the outer lumen of the gas conduit. An oxygen source is attached to the inner lumen and a vacuum pump to the outer lumen of the gas conduit, thus drawing oxygen through the hollow fibers. Devices tested clinically ranged in membrane surface area from 0.21-0.52 m^2. The hollow fiber membranes of the IVOX are crimped along their length, a process which permanently bends a straight fiber in the pattern of a sine wave. The crimping provides an opportunity for secondary currents around the fibers. Otherwise, the device sits in the central venous system and is dependent upon passive flow past the fibers to promote gas exchange. The fibers are not constrained and randomly assume their position once placed in the venous system. The polypropylene microporous hollow fiber membranes of the IVOX have an ultra-thin siloxane coating which functions as a true membrane. It is permeable to oxygen and carbon dioxide but impermeable to water, thus preventing the membrane pores from being subject to plasma leakage. A second coating is applied to all components of the IVOX and is a covalently bonded heparin derivative that is intended to increase the thrombo-resistance of the device. The intravascular oxygenator (IVOX) is the only intravenous device to have undergone Phase I and Phase II human clinical trials in the early 1990's.[50] The Phase I trials established the safety for introducing an intravascular oxygenator in humans, and the Phase II trial examined the clinical efficacy and gas exchange performance for this device. A total of 160 patients from the United States and Europe were studied. Criteria for inclusion or exclusion in the Phase II trial are given in Table 6.2. Once entry criteria were met, patients underwent a right internal jugular or femoral vein cut-down for device implantation. The largest size IVOX (0.21-0.51 m^2 membrane surface area) was chosen for implantation according to the vena cava size determined by ultrasound and the suitability of the access vein. The IVOX was furled during insertion and guided over a wire into position in the inferior vena cava, right atrium, and superior vena cava where unfurling occurred to fully expose the hollow fiber membranes to the returning venous blood. Heparinization (ACT 180-200 sec) was maintained during use of the device. After activation of the IVOX, attempts were made to reduce FIO_2 and minute ventilation as long as blood gases could be maintained with arterial oxygen saturations over 90%.

Table 6.2. Criteria for IVOX trial

Inclusion	
	FI_{O_2} 0.50 for 24 h or more with P_aO_2<60 mm Hg and one or more of the following:
	Positive end-expiratory pressure ≥10 cm H_2O
	Peak inspiratory pressure ≥45 cm H_2O
	Mean airway pressure ≥30 cm H_2O
	Minute ventilation >150 ml/min per kg with P_aCO_2>40 mm Hg
Exclusion	
	Uncontrolled multiple organ failure or patient in extremis
	Contraindication to systemic anticoagulation
	Uncontrolled bacteremia/fungemia
	Low cardiac output refractory to inotropes
	Lack of usable access vein (jugular or femoral)
	Existence of thrombi in major veins or vena cava
	Abnormal anatomy of the access veins or vena cava

The IVOX clinical trials confirmed earlier animal experiments and proved the feasibility of extended intravenous respiratory gas exchange in severe acute respiratory failure patients. In some patients, peak O_2 and CO_2 transfer rates varying between 40-70 ml/min were noted. During IVOX utilization, some clinical trial patients showed improvements in blood gas partial pressures and the ability to reduce the intensity of mechanical ventilation. The IVOX functioned in some patients for weeks without adverse effects. In these severely ill patients with acute respiratory failure, 60% survived to have the device removed, but only 30% improved to a point where mechanical ventilation could be discontinued. These same patients were hospital survivors and were discharged for an average 30% survival rate. Further trials of the IVOX were not pursued. Nevertheless, as the first and only clinical trial of an intravenous oxygenator, the IVOX provided valuable evidence that gas exchange (O_2 and CO_2) occurs in humans, but at a level that at the very best met only 30% of patients needs and was frequently not reproducible. Those involved in the clinical trial of the IVOX felt that in order to be clinically useful, an intravenous respiratory assist device would have to supply 50% of basal metabolic needs, be relatively easily insertible with minimal bleeding, and demonstrate consistent and reproducible gas exchange in patients with acute respiratory failure. These recommendations for improvements have been instrumental in our approach to designing devices dedicated to gas exchange in the venous system.

The Hattler Respiratory Support Catheter

The Hattler Respiratory Support Catheter or Hattler Catheter (HC) is an intravenous hollow fiber membrane gas exchange device intended for support of the acutely compromised lung. The catheter is introduced at the common femoral vein or internal jugular vein site and placed within the venous system, spanning the superior vena cava, right atrium, and inferior vena cava, as illustrated in Figure 6.4. A console outside the body connected to an exterior fitting of the Hattler Catheter provides a sweep gas flow of 100% O_2 through the hollow fiber membranes of the device. Early prototypes (Fig. 6.2) exchanged O_2 and CO_2 at levels that were considered too low to be of any clinical significance. To enhance gas exchange, a mechanism to control blood flow past the hollow fibers

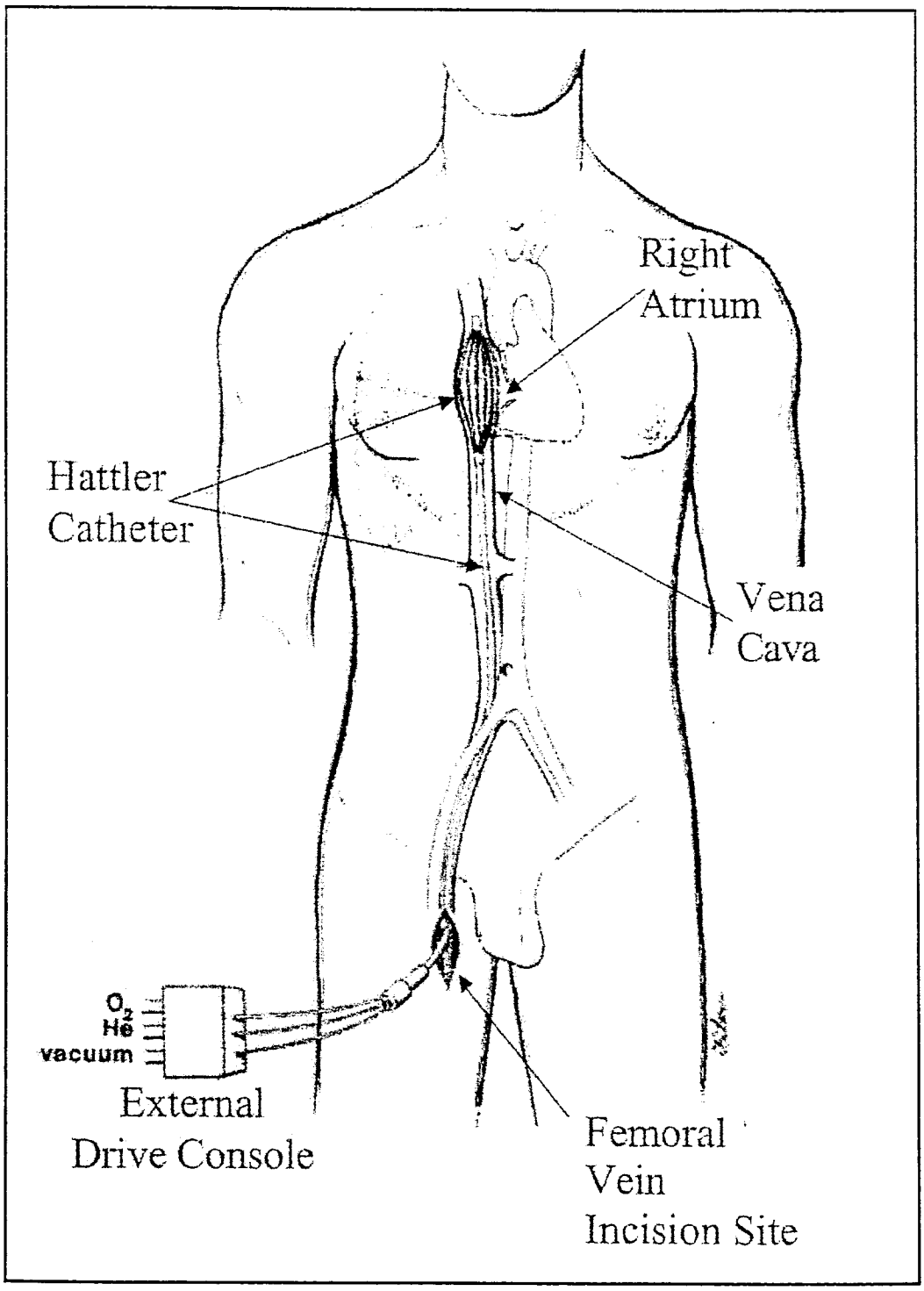

Fig. 6.4. Insertion and placement of the Hattler Catheter in the venous system. An external drive console provides a vacuum for driving sweep gas flow through the catheter and also pulsates the balloon with helium gas.

positioned in the vena cava was developed and consisted of a centrally placed balloon, around which the hollow fibers were circumferentially mounted. Inflation and deflation of the balloon created secondary flow profiles around the fibers. A shift in flow direction relative to the fibers from one that was predominantly parallel at zero balloon pulsation to one that was substantially transverse at 60-120 beats/minute was also noted.[16]

Biocompatibility of the HC is dependent on reducing shear stress and the potential for blood clotting and fibrin and cellular deposition on the surface of the hollow fiber membranes. A heparin bond linked to a < 1 μm thick siloxane coating covering the pores of the hollow fiber membrane (true membrane) has been used to enhance biocompatibility at the blood-membrane interface. In addition, early work in our laboratory has demonstrated that nitric oxide, as part of the sweep-gas within the hollow fibers, markedly diminishes cellular and platelet deposition on the membrane surface.[51] Other than the use of specialized coatings and controlling the composition of the oxygen mixture being vacuumed through the hollow fibers, a general principle applied to the design of the Hattler Catheter has been to minimize shear stress as a means of promoting biocompatibility. Flow in the vena cava is largely laminar where shear stresses occur because adjacent fluid layers travel at different speeds. Fluid in the center of the stream moves more quickly than fluid near the vessel wall. Therefore, shear rate is highest at the wall, the point of maximum shear being where blood cells adjacent to the wall are not moving and lowest at the center where friction is minimal. Flow velocity profiles visualized in the laboratory have shown that balloon pulsation can disrupt the layer of fluid next to the vessel wall (area of high shear stress), therefore reducing overall shear and potential damage to the formed elements of blood.[16] In addition, since, for maximum efficiency, the Hattler Catheter depends on blood flowing freely around the fibers where the blood is captured and directed towards the fibers by balloon pulsation, very low pressure drops (2-3 mm Hg) have been noted in large animal studies. By reducing the pressure drop, a reduction in shear at the same flow rates is noted, which promotes overall biocompatibility.

The initial fibers employed with this device in our research laboratories were not constrained and consisted of up to a thousand hollow fiber membranes, each floating within the blood. Testing in vivo and in vitro, demonstrated that gas exchange with balloon pulsation and active mixing had improved significantly. However, results with identical devices (same membrane surface areas) tested under identical conditions frequently varied significantly. The tendency of free fibers to clump together in bundles soon became apparent, especially when testing in blood. The end result of clumped fibers was a decrease in effective membrane surface area, as fibers in the center of each clump were not exposed to blood. An increase in the shunt fraction past the device would therefore occur with a decrease in gas exchange efficiency. Clumping, as a random, noncontrolled process occurred also with crimped fibers and could only be overcome by changing the hollow fiber membranes used with the device from nonconstrained, free fibers to fully constrained hollow fiber mats. The present configuration of the Hattler Catheter is depicted in Figure 6.5. The balloon occupies a central position and is surrounded by concentric layers of hollow fiber membrane mats that are potted into proximal and distal manifolds at each end of the device. The functioning components of the device sit at the end of a catheter through which 100% oxygen flows to the proximal manifold and is vacuumed from the distal manifold. A separate port provides helium to the balloon and is driven by a console capable of completely inflating and deflating the balloon at 300-600 beats/min. The device is inserted at present through a cut-down on the common femoral or internal jugular vein. When positioned, it occupies the inferior vena cava, right atrium, and superior vena

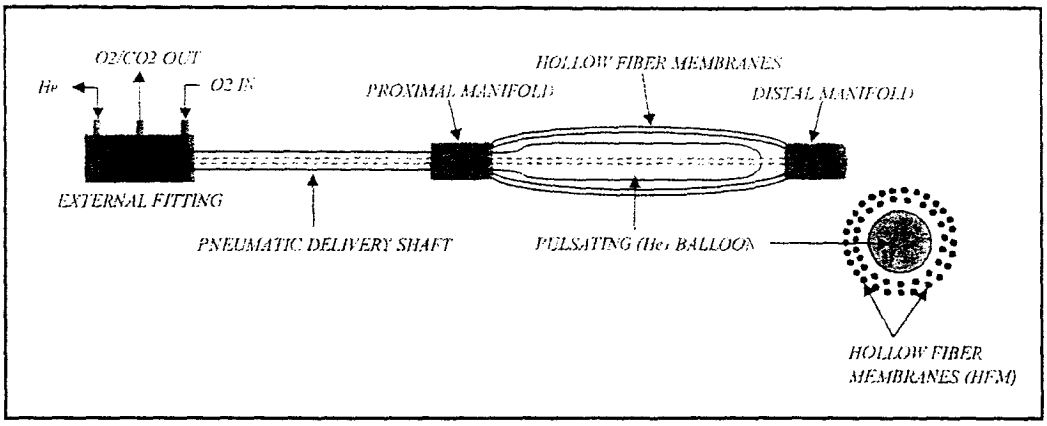

Fig. 6.5. Configuration of the Hattler Catheter. A pulsating balloon resides within the hollow fiber bundle, which is made using fiber fabric. The pneumatic delivery shaft directs the flow of incoming and outgoing sweep gas to the fibers and the oscillating flow of helium to the balloon.

cava. Reduction in the size of the catheter without losing gas exchange efficiency will permit percutaneous insertion in the future. In cases other than severe acute respiratory failure there exists the possibility that the ventilator can be dispensed with altogether. Since the resting CO_2 production of a 70 kg adult is approximately 240 ml/min, the majority of CO_2 can be readily removed by an intravenous respiratory assist catheter. Breathing for CO_2 removal will be reduced proportionally, leading to a reduction in tidal volume, peak inspiratory pressures, and the respiratory rate. In the extubated awake patient, this level of alveolar ventilation can lead to arterial hypoxemia but a small increase in the inspired FIO_2 should maintain normal alveolar oxygen concentrations. The ultimate effect on arterial oxygen tension however would depend on the degree of pulmonary arterio-venous shunting which becomes more severe with prolonged ventilatory support. This underscores the fact that the earlier a respiratory assist catheter is inserted the better the chance for a beneficial effect as it relates to both CO_2 removal and oxygenation. From a different perspective, the ability of the intravenous respiratory assist catheter to increase its CO_2 removal capacity as venous PCO_2 rises under the influence of a reduced tidal volume is therefore important if the device is to be used to its full potential. The bioengineering principles that have been utilized in arriving at our present state of development are discussed in the following section.

Basic Principles of Gas Exchange in the Hattler Catheter

The fundamental exchange units of the Hattler Respiratory Support Catheter are the hollow fiber membranes that compose its fiber bundle. Standard blood oxygenators used clinically during cardiopulmonary bypass employ thousands of these same fiber membranes in ensemble arrangements or bundles that vary among the oxygenator designs. Hollow fiber membranes are essentially small polymer tubes, typically with outer diameters from 200 to 400 μm, and with microporous walls of 20 to 50 μm thickness (see Fig. 6.6). The pores within the walls have characteristic dimensions typically below about 0.1 μm, and the porosity or volume fraction of pores within the fiber wall can vary from about 30% to 50%. The polymers selected for oxygenator fiber membranes are hydrophobic, or liquid repelling, so that normally the pores remain gas filled and allow for ready diffusion of respiratory gases through the fiber wall.

The hollow fibers used in the Hattler Catheter exchange gas with blood following the same general principles as in other artificial lungs composed of fiber membranes. Oxygen gas flows through the insides of the hollow fibers while blood flows on the outsides of the hollow fibers through the interstices of the hollow fiber bundle. Oxygen then moves from the gas to the blood side of the membrane, while carbon dioxide moves from the blood to the gas side of the membrane, both down their respective diffusion gradients determined by the partial pressures of these gases on both sides of the membrane (i.e., the walls of the hollow fibers). The gas exchange permeance * or mass transfer coefficient, K, of an artificial lung represents the rate of gas exchange, for either O_2 or CO_2, normalized to fiber surface area and to the gas partial pressure difference driving exchange. Considering O_2 as the species of interest, the gas exchange permeance is related to the overall O_2 exchange rate, $\dot{m}_{O_2}$, by

$$\dot{m}_{o_2} = K_{o_2} A_s \left[(\overline{Po_2})_g - (\overline{Po_2})_b \right], \qquad \text{(Eqn. 6.1)}$$

where $(\overline{Po_2})_g$ and $(\overline{Po_2})_b$ are the *average* O_2 partial pressures in the gas and blood phases, respectively, contacting the membrane, and A_s is the total surface area of the fiber membranes. Accordingly, the gas exchange permeance provides a measure of the gas exchange efficiency of an artificial lung.[52] For the Hattler Catheter, gas permeance has been a useful index for characterizing device performance and tracking progress during device development. The gas exchange permeance of an artificial lung for CO_2 can be defined through a similar relationship.

Overall gas exchange for O_2 or CO_2 in an artificial lung like the Hattler Catheter is dictated by diffusional resistances encountered serially as each species moves from the gas to blood phase, or vice versa. Indeed, permeance and resistance are inversely related, and hence the overall transfer resistance of an artificial lung is given by $1/K$. This overall transfer resistance has two principal components:

$$\frac{1}{K} = \frac{1}{K_m} + \frac{1}{K_l}, \qquad \text{(Eqn. 6.2)}$$

where $1/K_m$ represents the diffusional resistance of the hollow fiber membranes and $1/K_l$ represents the transfer resistance associated with diffusional boundary layers on the liquid-side (i.e., blood-side) of the fibers, which will be further discussed below. The permeances K_m and K_l are the membrane and liquid-side gas permeances of the artificial lung, respectively. The general relationship of the membrane and liquid-side resistances to gas exchange in artificial lungs and in the Hattler Catheter is illustrated in Figure 6.7. The general gradients in partial pressure associated with these resistances are also illustrated for the case of O_2. First, transfer resistance in the gas phase within the fibers is considered negligible because of substantial bulk gas flow through the fiber lumens, which minimizes the Po_2 gradients within the fiber. Most of the transfer resistance and hence the gradient in Po_2 is associated primarily with the liquid-side diffusional boundary layer, and second-

* "Permeability" is often used in the perfusion literature in place of "permeance" to describe gas transfer features of blood oxygenators or the membranes composing them. "Permeability" is more correctly used to describe a *material* property of polymers relating to their gas transmissibility, and is independent of geometrical configuration and thickness. "Permeance" is the most appropriate term used to describe the gas transmission properties of a given material or system with a given geometrical configuration and membrane thickness.

arily with diffusion through the membrane itself. Thus, liquid-side and membrane gas permeances dictate overall gas exchange in the Hattler Catheter and represent serial transport processes, in which their resistances add directly to determine overall resistance (Eq. 6.2). The serial resistance relationship means that the overall gas exchange permeance, K, is always less than the smallest of the permeances, K_m and K_l. More simply, the transport process with the smallest permeance or largest resistance controls gas exchange in the Hattler Catheter, as it does in any artificial lung. In what follows, we introduce some basic transport concepts to help understand the nature of the membrane and liquid-side gas permeances of an artificial lung like the Hattler Catheter.

Gas Permeance of Microporous Hollow Fibers

Microporous hollow fiber membranes are the most common hollow fibers used for artificial lung design, especially in the standard blood oxygenators used in cardiopulmonary bypass. Microporous fiber membranes have fixed submicron pores within the wall that are contiguous from outer to inner lumen (see Fig. 6.6), and gas exchange occurs by gas diffusion through these pores. Generally, the polymer material does not dictate the exchange performance of the fiber as much as the pore characteristics and the fiber wall porosity, as will be further discussed below. An important polymer-related property of hollow fibers is their hydrophobic versus hydrophilic nature. Hydrophobic fibers are used in artificial lungs because they prevent intrusion of blood plasma into the fiber pores under normal conditions, a process known as plasma or liquid wetting.[53,54] The principal manufacturers of microporous hollow fiber membranes for artificial lungs are Celgard (Charlotte, NC), Akzo-Nobel in Germany, and Mitsubishi Rayon in Japan. Currently, the Hattler Catheter under research development uses the Celgard X30-240 microporous fiber, with slit pores of 0.03 μm by 0.2 μm, and a nominal porosity of 40%. The Hattler Catheter made for ultimate human implantation will use similar microporous hollow fibers modified to prevent plasma wetting and to improve biocompatibility, as will be discussed below.

The resistance to gas exchange offered by a microporous hollow fiber membrane, and its potential effect on overall gas exchange in an artificial lung like the Hattler Catheter, depends on the permeance, K_m, of the fiber membrane (see Eqs. 6.1 and 6.2). Fiber permeance values, however, are not usually reported in the specifications provided by the fiber manufacturers. A likely reason is that K_m values for microporous hollow fibers are relatively large, $K_m >> K_l$, so that membrane resistance is negligible compared to liquid-side resistance in an artificial lung, thus obviating the need for a design specification and value for K_m. A simple theoretical relation can be derived to estimate K_m values for microporous fibers. Gas diffusion through the pores of oxygenator fibers is governed by Knudsen diffusion, where interactions of gas molecules with the pore walls dominate molecular motion.[55] Assuming Knudsen diffusion, a microporous membrane of porosity, ε, composed of idealized cylindrical pores of diameter, d_p, would have a membrane permeance given by:

$$K_m = \varepsilon \frac{2}{3} \frac{d_p}{\tau h} \sqrt{\frac{2}{\pi MRT}}, \qquad \text{(Eqn. 6.3)}$$

where h is the fiber wall thickness, τ is the pore tortuosity, M is the molecular weight of the gas, R is the gas constant, and T is absolute temperature. For parameter values approximating the Celgard X30-240 fiber: ε = 0.40, d_p = 0.03 μm, and h = 30 μm, the estimated membrane permeance* for O_2 at 37° C is $K_m = 2.3 \times 10^{-2}$ ml/(cm^2•s•cm Hg), assuming a

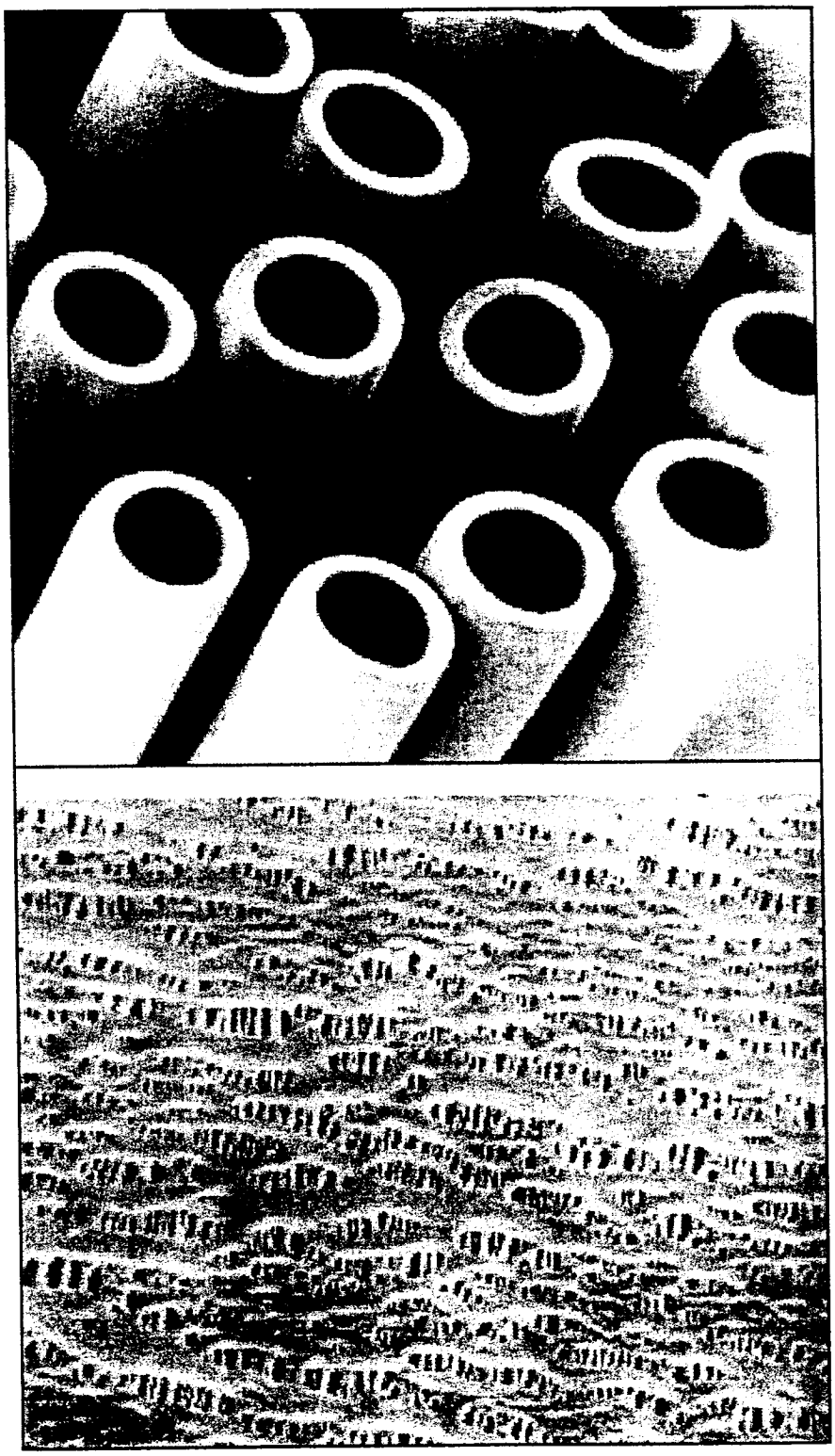

Fig. 6.6. Scanning electron micrograph of microporous hollow fiber membranes (top panel). The walls of hollow fibers contain submicron size pores (bottom panel) for ready transmural diffusion of respiratory gases.

pore tortuosity of $\tau = 3$. For these same conditions, the estimated membrane permeance for CO_2 is $K_m = 2.0 \times 10^{-2}$ ml/(cm^2•s•cm Hg).

A membrane permeance of $K_m \sim 10^{-2}$ ml/(cm^2•s•cm Hg) represents an enormous gas exchange capacity which is never realized in an artificial lung. For example, an artificial lung with 0.5 m^2 of membrane area, as in the largest anticipated Hattler Catheter device, and with a 700 mm Hg P_{O_2} difference held between the gas and blood phases, could hypothetically transfer approximately 200 l/min of O_2 across the membrane if K_m dictated exchange. This exchange rate is not only much greater than needed to saturate blood flowing at physiological flow rates, but is several thousand fold greater than actually occurs because the predominant resistance to gas exchange resides within the blood phase, in the diffusional boundary layers adjacent to the fiber wall surfaces. Hence, the overall gas exchange permeance of a Hattler Catheter, as for any artificial lung, is substantially less than the permeance of the hollow fiber membranes comprising the device.

The permeance of microporous hollow fibers can be measured with the fibers immersed in a gas rather than liquid phase (i.e., a gas-gas system), so that liquid-side boundary layers are not present and all the transfer resistance is associated with the membrane. If Knudsen diffusion conditions exist within the pores, convective gas flow across the fiber wall due to a transmural pressure difference can be ignored.[55] Kamo et al.[56] measured the oxygen permeance of the Mitsubishi KPF fiber in a gas-gas system and reported a $K_m = 6.7 \times 10^{-2}$ ml/(cm^2•s•cm Hg). Lund[57] determined K_m values of 1.72×10^{-2} and 1.47×10^{-2} ml/(cm^2•s•cm Hg) for O_2 and CO_2, respectively, at room temperature for the Celgard X30-240 fiber. In the Lund studies, the measured K_m were independent of the absolute pressure difference applied across the fiber walls, indicating that convective gas flow through pores was not important and that Knudsen diffusion dominated transfer. The ratio of membrane permeance to CO_2 versus O_2 was 1.47/1.72 = 0.85, which is also consistent with Knudsen diffusion of these gases through the fiber (see Eq. 6.3). Thus, even with microporous fibers immersed within a gas rather than liquid phase, gas movement across the fiber wall occurs by Knudsen diffusion, the same mechanism that would occur if the fibers were immersed in a liquid. Under these conditions fiber permeance measured in a gas-gas system should reflect that when fibers are immersed within a liquid.

Can membrane permeance be reduced or otherwise changed by the fibers being immersed in a liquid, especially a more complex liquid like blood, in which proteins and cellular elements may adsorb to the fiber surface and affect membrane permeance? While an interesting question, the large K_m of microporous hollow fibers makes it difficult to measure K_m when the fibers are immersed in a liquid phase (i.e., a gas-liquid system). In a gas-liquid system, the K_m measurement must account for the liquid-side permeance, K_l, due to diffusional boundary layers on the fiber surfaces, even in the presence of substantial liquid-side mixing. Lund et al.[58] developed a diffusion chamber to measure hollow fiber membrane permeance in various liquid media, including water, plasma, and blood. By systematically increasing the stirring rate of the liquid bathing the fibers, the effect of the liquid boundary layer can be sequentially reduced, and a value of K_m can be estimated by extrapolating to an infinite level of stirring. Lund[57] demonstrated that K_m can be determined in this manner provided its value is no more than 10 times the maximum K_l engendered by the applied mixing. In the diffusion chamber developed by Lund et al., the largest K_l value reached at a stirring rate of 3000 RPM was less than 1×10^{-3} ml/(cm^2•s•cm Hg) for CO_2 and less than 1×10^{-4} ml/(cm^2•s•cm Hg) for O_2. Hence, reliable determina-

* The units used for fiber permeance are conventional, where gas volume is referenced to STP conditions.

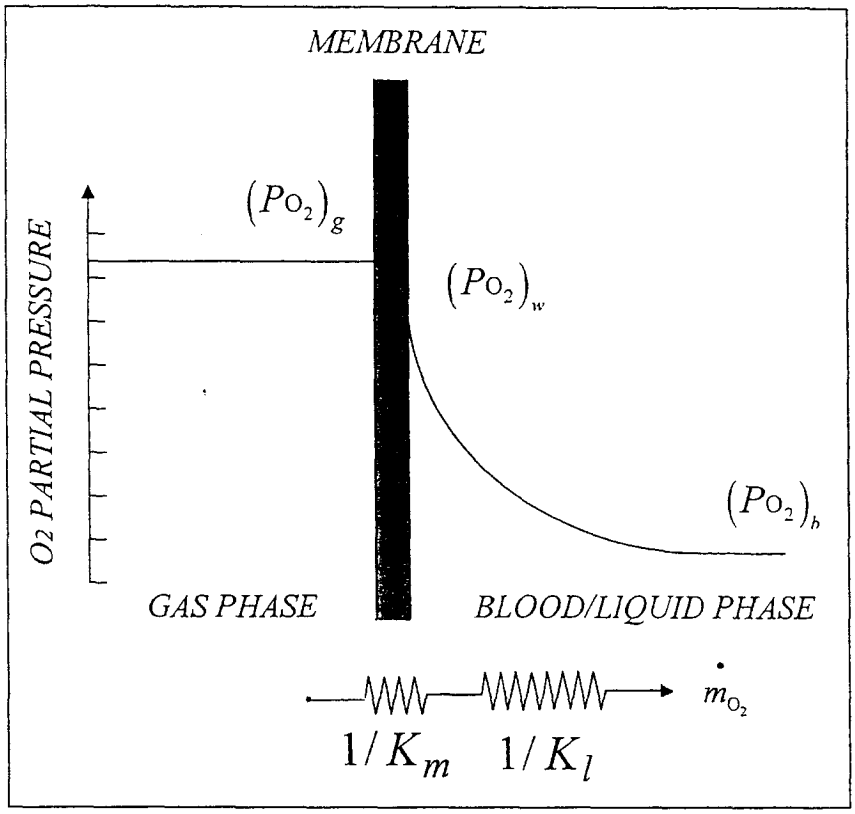

Fig. 6.7. Membrane and liquid-side gas permeances, K_m and K_l, respectively, dictate gas exchange from the gas phase flowing inside hollow fibers to the blood phase flowing outside the fibers. The "membrane" refers to the walls of the hollow fibers composing an artificial lung.

tion of a microporous fiber K_m in the gas-liquid system would be difficult for CO_2 and impossible for O_2 unless liquid immersion causes substantial reductions in K_m. Plasma wetting of the fiber pores is one potential mechanism for substantially reducing the membrane permeance of microporous hollow fiber membranes immersed in blood. Plasma wetting and the composite hollow fibers used to prevent plasma wetting are discussed later, after the principal concepts underlying the liquid-side permeance of the Hattler Catheter are introduced.

Liquid-Side Boundary Layer Permeance

Fluid elements flowing adjacent to a stationary surface experience a decrease in velocity, eventually becoming stagnant immediately at the surface. The liquid or blood-side permeance of an oxygenator, K_l, accounts for gas diffusion away from or towards the fiber surface through these convection-poor and imperfectly-mixed boundary layers adjacent to the fiber surface. The gas species must traverse the boundary layer by molecular diffusion before it can be exposed to sufficient convection to be carried away by the flowing stream of blood past the fiber. The boundary layer concept is illustrated in Figure 6.8, which shows the diffusional boundary layer associated with uniform laminar flow past a flat membrane surface. The boundary layer adjacent to the surface, where transport occurs predominantly by diffusion, grows with distance along the surface in the flow direction. Even a submicron-sized diffusional boundary layer can result in a K_l appreciably below the

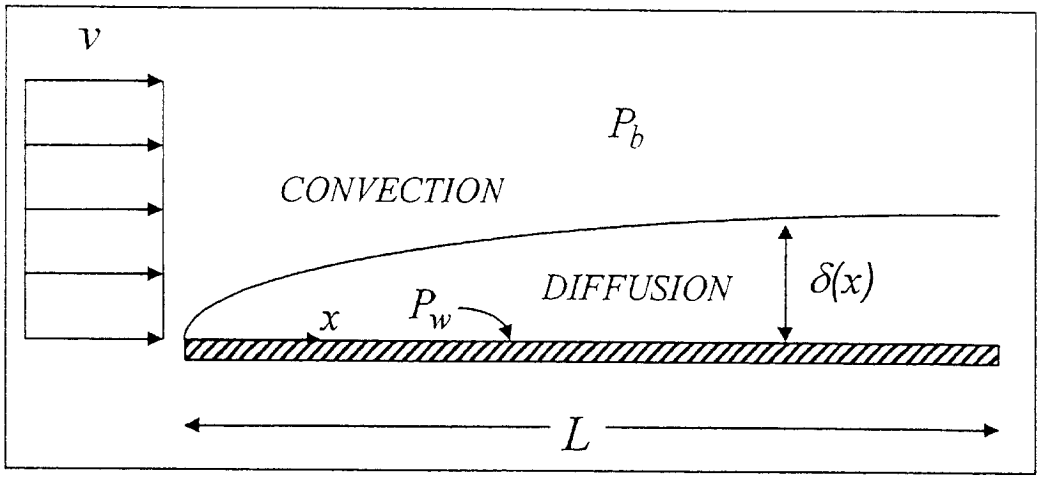

Fig. 6.8. Illustration of growing diffusional boundary layer on flat membrane surface with convective flow past the surface. Transfer to and from the membrane surface is predominantly by diffusion within the boundary layer, while convection by bulk flow predominantly carries gas species outside the boundary layer. (υ=fluid velocity past membrane surface; L=length of surface along direction of flow; $\delta(x)$=boundary layer thickness with position, x, along membrane surface; P_b and P_w=gas partial pressures in bulk fluid stream and at the membrane surface, respectively.)

K_m for a microporous hollow fiber membrane, and can limit overall gas exchange, as will be further discussed below.

The permeance of a liquid-side boundary layer can be expressed generally as

$$K_l = \frac{\alpha_l D_l}{\delta_{bl}}, \qquad \text{(Eqn. 6.4)}$$

where α_l and D_l are the effective solubility and diffusion coefficient, respectively, of the diffusing gas in the liquid phase and δ_{bl} is the average boundary layer thickness (more specifically, the harmonic-mean thickness). Equation 6.4 is exact for simple liquids like water, but also describes gas diffusion within blood if the solubility coefficient effectively accounts for increased solubility due to hemoglobin binding for O_2 or storage by the bicarbonate system for CO_2. Essentially, the liquid boundary layer thickness, δ_{bl}, represents an average distance that O_2 must diffuse away from the fiber before being swept away by the bulk flow of blood. For CO_2, δ_{bl} represents the average distance for diffusion to the fiber surface after being carried to the fiber by the flow of blood. The value of δ_{bl} depends principally on the local-scale interaction between diffusional fields and flow dynamics in the blood phase subjacent to the fibers, the latter being complicated in the Hattler Catheter. Active *mixing* of blood by the pulsating balloon in the Hattler Catheter drives additional convective blood flow across the fibers to increase convective mixing, minimize the diffusional boundary layer thickness, and increase the liquid-side gas permeance, K_l.

How the liquid-side permeance depends on boundary layer growth and thickness has important implications for the design of artificial lungs like the Hattler Catheter, and the theory for the diffusional boundary layer arising along a flat surface (as in Figure 6.8) provides important insight. The diffusional boundary layer on a flat surface grows as the square root of distance, x, along the surface according to:

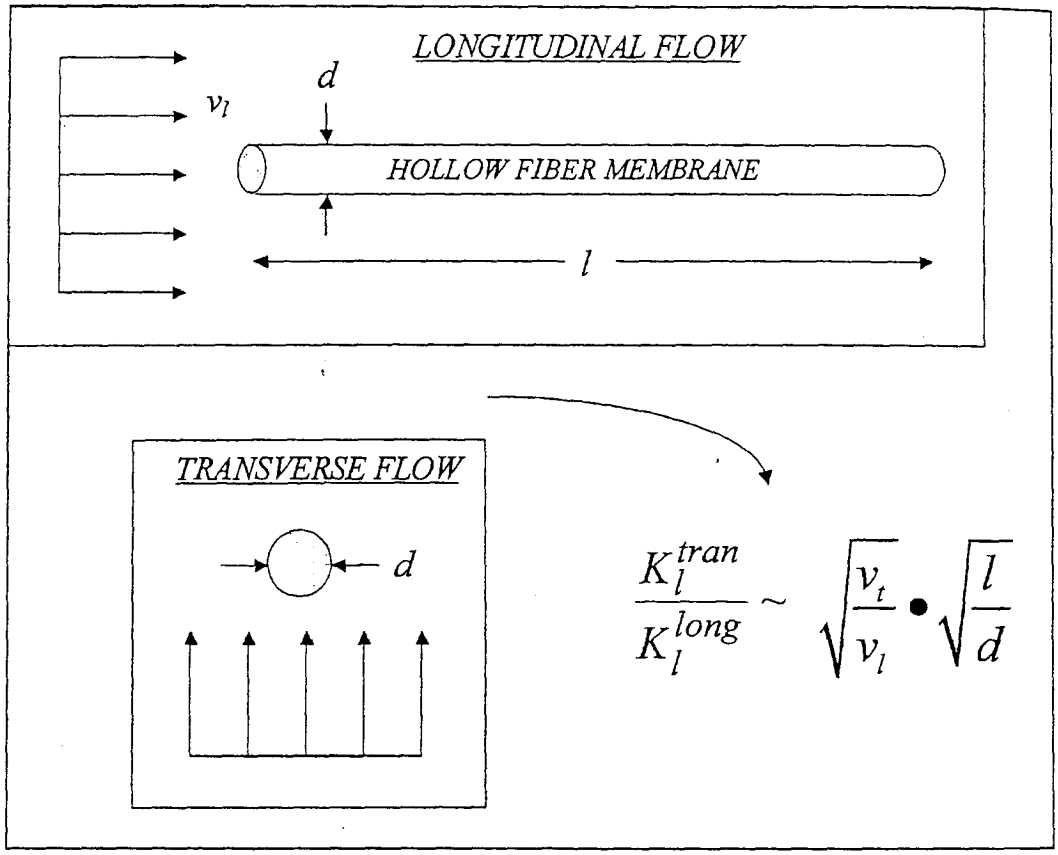

Fig. 6.9. Comparison of longitudinal flow (parallel flow) and transverse flow (perpindicular or cross flow) past hollow fibers. Diffusional boundary layers are smaller in cross-flow than in parallel flow leading to greater liquid-side gas permeance, K_l. (υ_t and υ_l=fluid velocity past fiber in either transverse or longitudinal flow direcions, respectively; d=fiber outer diameter; l=fiber length.)

$$\delta_{bl}(x) \approx \left(\frac{\nu}{D_l}\right)^{1/6} \sqrt{\frac{D_l}{v_b} x}, \qquad \text{(Eqn. 6.5)}$$

where ν is the liquid kinematic viscosity, D_l is the gas diffusion coefficient in the liquid and v_b is the bulk flow velocity past the surface, essentially that of the fluid elements undisturbed by the surface. An important implication of boundary layer growth is that considerable advantage can be gained from orienting the exchange surfaces (i.e., the hollow fibers) perpendicular rather than parallel to the bulk convective blood stream (Fig. 6.9). With perpendicular or *transverse* flow to the hollow fibers, the fiber surface along the flow direction scales as the diameter, d, of the fibers, while that with parallel or *longitudinal* flow to the hollow fibers scales as the length, l, of the fiber, as illustrated in Figure 6.9. Accordingly, for a given gas species and liquid-side velocity, boundary layer theory (i.e., Eqs. 6.4 and 6.5) predicts that K_l for transverse versus longitudinal flow would scale as:

$$\frac{K_l^{tran}}{K_l^{long}} \approx \sqrt{\frac{l}{d}}. \qquad \text{(Eqn. 6.6)}$$

For fiber lengths and diameters characteristic of an intravenous artificial lung like the Hattler Catheter, with $l/d \sim 1000$, Equation 6.6 suggests that transverse blood flow, or cross-flow to the hollow fibers, improves gas exchange permeance approximately thirty-fold.

The pulsating balloon in the Hattler Catheter improves gas exchange partly by generating more cross-flow to the fiber membranes than might otherwise exist in the vena cava and thereby capitalizing on the mass transfer advantages afforded by cross-flow. The boundary layer paradigm also suggests that balloon enhancement of gas exchange will increase as the square root of balloon pulsation, since the (balloon-engendered) flow velocity depends linearly on balloon pulsation rate, and boundary layer thickness depends inversely on the square root of flow velocity.

The liquid-side gas permeance, K_l, associated with diffusional boundary layers usually limits gas exchange in artificial lung devices, and it does so in the Hattler Catheter. This is not surprising if one considers that K_l for O_2 diffusing in water through a 10 μm thick boundary layer is about 9 x 10^{-6} ml/(cm^2•s•cm Hg) (at 37°C for O_2 in water: α_l = 3.2 x 10^{-4} ml/(cm^3•cm Hg) and D_l = 2.8 x 10^{-5} cm^2/s). The K_l in blood may be several times greater due to increased O_2 solubility provided by hemoglobin, but still remains in the range of 10^{-5} ml/(cm^2•s•cm Hg). The K_l value for CO_2 diffusing through a boundary layer of the same thickness is on the order of 10^{-4} ml/(cm^2•s•cm Hg). In contrast, a microporous hollow fiber membrane has a K_m value in the range of 10^{-2} ml/(cm^2•s•cm Hg), as discussed previously. Thus, a diffusional boundary layer of just 10 μm, only a fraction of the fiber size, yields O_2 and CO_2 liquid-side permeances appreciably below those of the fiber membrane, hence, $K_l << K_m$. Moreover, increasing K_l by generating smaller-scale mixing is difficult, even with rapid balloon pulsation in the Hattler Catheter. Thus, under normal conditions in an artificial lung and in the Hattler Catheter, the overall exchange permeance is dictated by the diffusional boundary layer, or

$$K \cong K_l, \qquad \text{(Eqn. 6.7)}$$

Only under conditions of substantially reduced K_m would the gas exchange permeance of the hollow fibers have an appreciable influence on overall artificial lung performance. Plasma wetting of the fiber pores is one potential mechanism for substantially reducing the membrane permeance of microporous hollow fiber membranes. For this reason, the permeance of fiber membranes assumes greater importance in the development of an implantable artificial lung like the Hattler Catheter, which must effectively resist plasma wetting. The fibers ultimately used in the Hattler Catheter will be composite hollow fiber membranes, with thin nonporous polymer coatings applied to the fibers to prevent plasma wetting. The nonporous polymer layer of a composite fiber reduces the membrane permeance substantially. If K_m becomes comparable to K_l the overall gas exchange permeance of the artificial lung will also be reduced (see Eq. 6.2). For these reasons, studying the membrane permeance of composite hollow fibers has been central to development of the Hattler Catheter. The following section further discusses membrane permeance in the Hattler Catheter in relation to plasma wetting and the use of composite hollow fibers designed to prevent wetting.

Composite Fiber Membranes and Membrane Permeance

Microporous fiber membranes are made from hydrophobic polymers (e.g., polypropylene) so that pores stay gas filled and membrane permeance remains high. Nevertheless, membrane permeance degrades significantly when these fibers are exposed to blood due to plasma wetting, whereby blood plasma infiltrates the microporous walls of hollow fibers. Plasma wetting is a common problem in the extended use of extracorporeal oxygenators,[53,54] which can lead to device failure within days. Plasma wetting results primarily from phos-

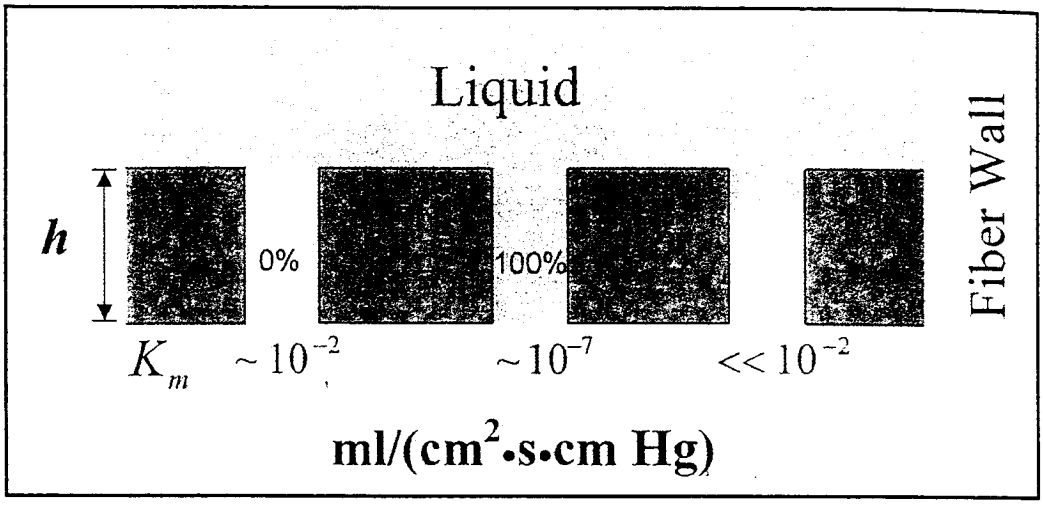

Fig. 6.10. Membrane permeance, *Km*, associated with dry (gas-filled) fiber wall pores versus liquid-wetted fiber wall pores. Pore wetting markedly reduces *Km*, even with partial wetting of fiber pores.

pholipids, lipoproteins and/or proteins in blood[53] which can adsorb onto the fiber polymer surfaces at the plasma interface, rendering the interface hydrophilic and allowing for wetting of the pores by either partial or complete plasma infiltration. In contrast, the membrane permeance of hollow fibers immersed in pure water has been shown to remain constant for days under flow and pressure conditions applicable to blood oxygenators, thus indicating that fiber pores remain gas filled in simple liquids like water.[59]

Liquid infiltration into gas filled pores markedly diminishes the membrane permeance, K_m, because rapid gas phase diffusion is replaced by diffusion in a liquid, as illustrated in Figure 6.10. For entirely liquid filled pores (i.e., complete wetting), the membrane permeance, K_m, is given by:

$$K_m = \varepsilon \frac{\alpha_l D_l}{\tau h}, \qquad \text{(Eqn. 6.8)}$$

where, α_l and D_l are the solubility and diffusion coefficient of gas in the liquid filling the pores, and ε, h and τ are the fiber wall porosity, thickness and pore tortuosity, which also affect the K_m of gas filled microporous fibers (see Eq. 6.3). Thus, complete wetting reduces K_m markedly because the gas diffusion coefficient in any liquid is substantially less than in a gas, and because the solubility of the gas in a liquid (i.e., the dissolved gas mass per unit mass of liquid) is small. A typical K_m value for a completely wetted fiber, assuming water-filled pores and the same fiber parameters used previously, is in the range of 10^{-7} ml/(cm^2•s•cm Hg) for O_2, a 100,000-fold decrease compared to K_m for gas-filled pores. This marked effect of wetting means that even partial liquid infiltration into fiber pores can significantly reduce K_m. In the previous example, a 1% penetration of liquid into the gas filled pores would reduce K_m to about 10^{-5} ml/(cm^2•s•cm Hg), still a marked reduction in membrane permeance compared to that if the pores were gas-filled. K_m in this situation would be comparable to liquid-side permeance, thus affecting overall gas exchange.

The fiber membranes selected for the Hattler Catheter, as for other implantable artificial lungs, must effectively resist plasma wetting and the associated reduction in gas exchange performance. Unlike extracorporeal artificial lungs, replacing the Hattler Catheter after plasma wetting is not feasible nor desirable. Although a strategy to resist plasma

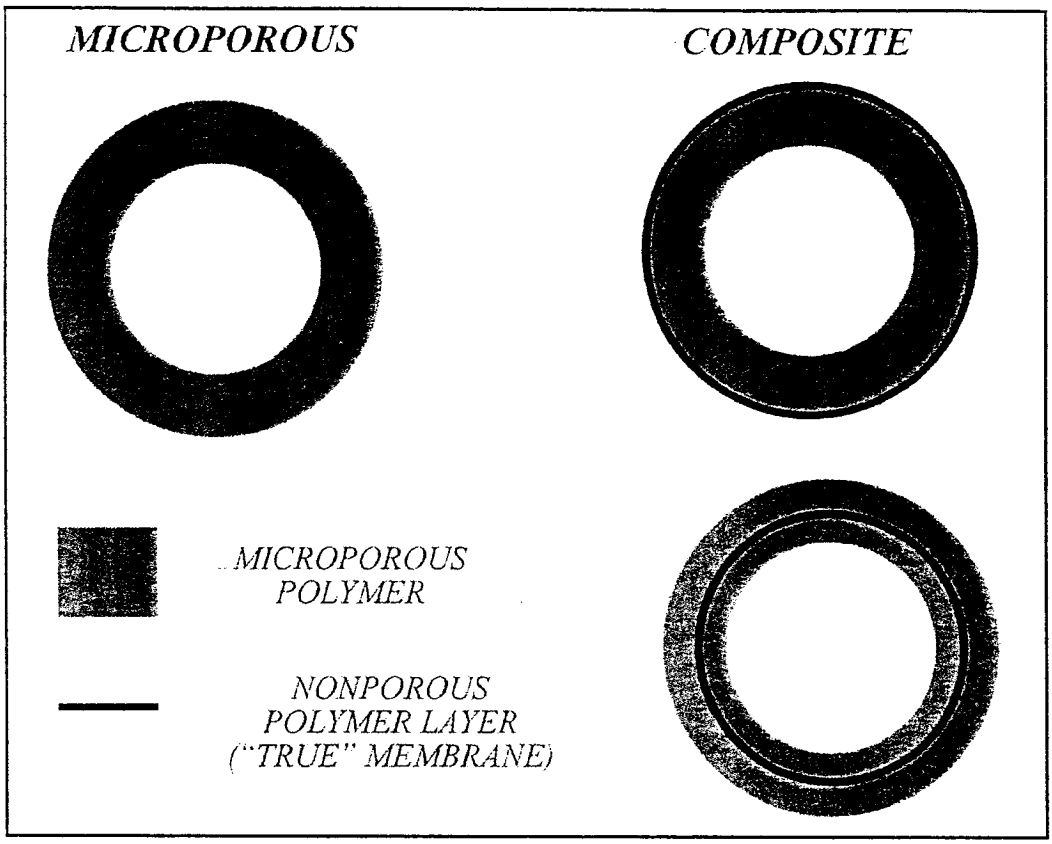

Fig. 6.11. Composite hollow fibers incorporate a nonporous polymer layer, or true membrane, with a microporous polymer wall to block fiber wetting. The microporous polymer provides structural support for the true membrane, which dictates diffusion through the fiber wall.

wetting might involve using fibers with reduced pore size, preventing plasma wetting requires using composite hollow fiber membranes. Composite hollow fibers incorporate a thin nonporous polymer layer, or "true" membrane that typically coats the outside of a microporous fiber membrane, as indicated in Figure 6.11. The nonporous polymer layer, if contiguous on the outside of the fiber, effectively blocks liquid intrusion into the microporous wall. Composite hollow fiber membranes are made by either coating an existing microporous fiber with a thin nonporous polymer (a true composite hollow fiber), or by modifying the fabrication of the microporous fiber itself to seal-off pores at the surface (an asymmetric hollow fiber). Figure 6.12 shows scanning electron micrograph images of a composite hollow fiber as compared to an asymmetric hollow fiber, both shown in cross-section of the outer fiber wall. Although asymmetric hollow fiber membranes have manufacturing advantages, the same polymer constitutes the nonporous and microporous sections of the fiber wall, and the nonporous polymer may not have suitable gas transmission properties. Conversely, composite hollow fibers can use highly permeable nonporous polymers for the true membrane, but layer contiguity and potential delamination become important issues. Figure 6.11 also illustrates a composite hollow fiber membrane with the true membrane sandwiched within the microporous wall, a composite fiber previously available from Mitsubishi Rayon (MHF fiber series). This composite fiber may prevent plasma seepage into the fiber lumen, but if partial wetting of the outer

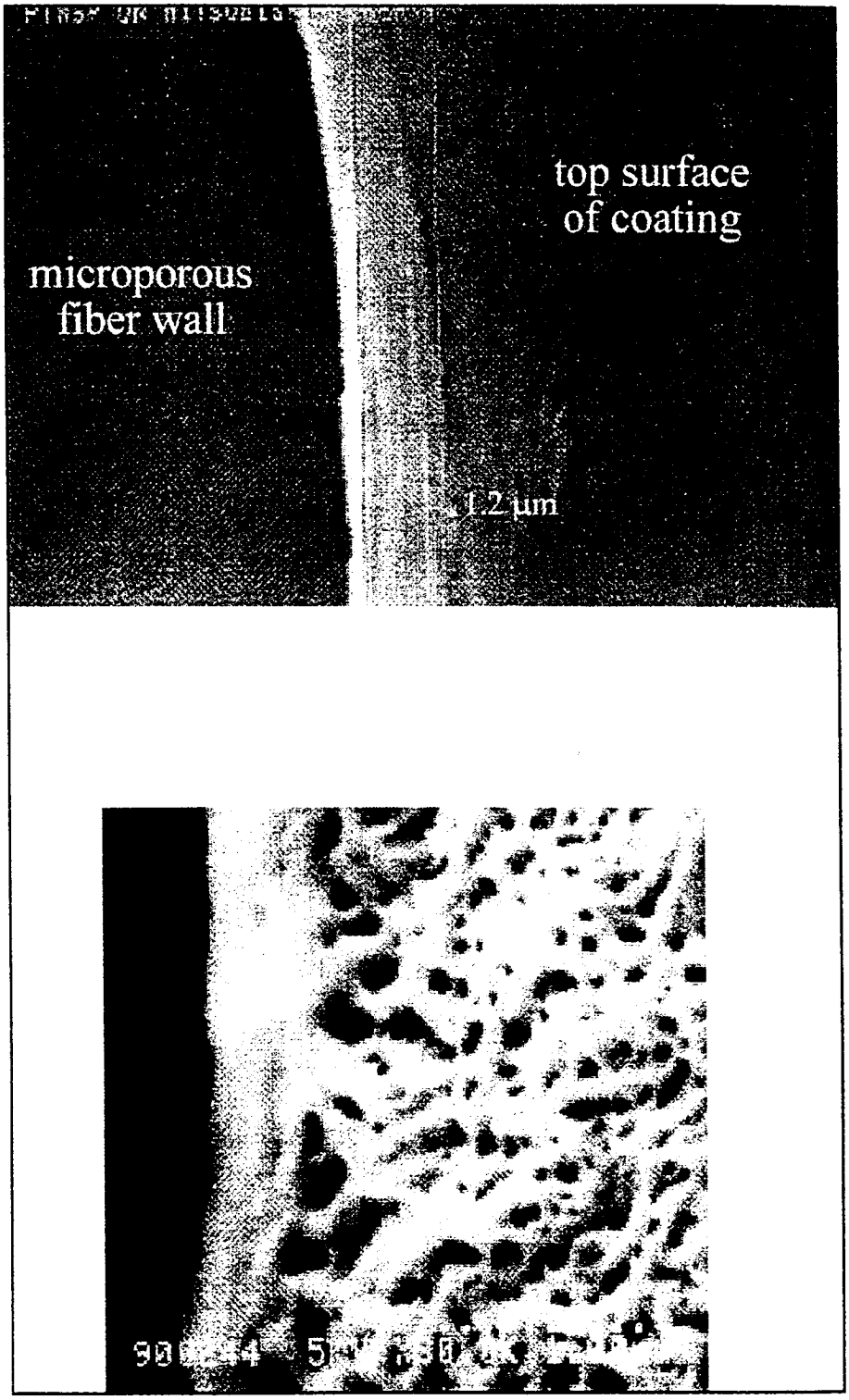

Fig. 6.12. Scanning electron micrographs showing showing cross-sections: the outer fiber wall for a composite (coated) hollow fiber membrane (top panel), and an asymmetric hollow fiber membrane (bottom panel).

microporous wall segment can occur, the membrane gas permeance will be substantially reduced, as described previously.

The very strategy meant to block plasma wetting in composite hollow fiber membranes diminishes membrane permeance, since the nonporous polymer layer presents an appreciable relative impediment to gas diffusion. Indeed, the membrane permeance of a composite hollow fiber is generally dictated by the true membrane, since nonporous or dense polymers have low gas permeances compared to the large permeance of the gas-filled microporous wall with which the nonporous polymer layer is in series. Like liquid layers, gas permeation across a nonporous polymer layer involves gas solubility within the polymer molecular matrix and subsequent diffusion through its matrix. Thus, the macromolecular properties of the polymer material used for the true membrane play a dominating role in membrane permeance. The membrane permeance of a composite hollow fiber is given by:

$$K_m = \frac{\alpha_p D_p}{\delta_p} = \frac{P_m}{\delta_p}, \qquad \text{(Eqn. 6.9)}$$

where α_p and D_p are the solubility and diffusivity of the gas within the dense polymer layer and δ_p is its thickness. Most often, polymer manufacturers report the *product* of polymer solubility and diffusivity, the polymer permeability, P_m, to specific gases rather than the solubility and diffusivity individually. Typical gas permeabilities of "normal" permeability polymers are in the range of a Barrier, which is the commonly used unit of polymer permeability, where 1 Barrier = 10^{-10} ml/(cm^2•s•cm Hg). Thus, according to Equation 6.9, the membrane permeance of a composite hollow fiber with a 1 μm thick layer of a 1 Barrier nonporous polymer is $K_m = 10^{-6}$ ml/(cm^2•s•cm Hg), a relatively small and potentially gas exchange limiting membrane permeance. Composite hollow fiber membranes suitable for artificial lung applications ideally require nonporous polymers with relatively high gas permeabilities in the range of 100 Barriers or greater, and which can be coated in stable contiguous layers in the range of 1 μm thickness or less. Many of the siloxane polymers, which have permeabilities of 100 Barriers or greater, have been and still remain attractive candidates for fabricating composite hollow fiber membranes.

The selection or development of an appropriate composite hollow fiber membrane for the Hattler Catheter requires a fiber K_m large enough compared to liquid-side gas permeance, K_l, so that the impact on overall gas exchange is minimal. Appropriate initial K_m target values can be estimated using a criterion that the transfer resistance offered by the fiber membranes be less than 10% of the overall gas transfer resistance, or in permeance terms: $K_m \leq 10K$. To use this criterion, the appropriate overall permeance, K, of the Hattler Catheter is estimated by rearranging Equation 6.1 and applying our design target for gas exchange for O_2 and CO_2 along with estimates of average gas-side and blood-side partial pressures. For example, targeting a gas exchange rate for O_2 and CO_2 of 125 ml/min with a 0.5 m^2 Hattler Catheter, and assuming the following gas and liquid-side partial pressures for O_2: $(P_{O_2})_g$ = 660 mm Hg and $(P_{O_2})_b$ = 40 mm Hg, and for CO_2: $(P_{CO_2})_g$ = 0 mm Hg and $(P_{CO_2})_b$ = 50 mm Hg, yields overall permeances of K_{O_2} = 7 x 10^{-6} ml/(cm^2•s•cm Hg) and K_{CO_2} = 8 x 10^{-5} ml/(cm^2•s•cm Hg). Thus, the adopted criterion for membrane permeance suggests target K_m values of:

$$K_m \geq 7\text{x}10^{-5} \text{ ml/(cm}^2\text{•s•cm Hg) for } O_2$$

$$K_m \geq 8\text{x}10^{-4} \text{ mlml/(cm}^2\text{•s•cm Hg) for } CO_2 .$$

Composite hollow fiber membranes with permeances appreciably below the target K_m will engender significant reductions in overall gas exchange performance of the Hattler Cath-

Table 6.3. Membrane permeance of candidate composite hollow fiber membranes

	K_m in ml/(cm^2•s•cm Hg)	
Fiber	**Oxygen**	**Carbon Dioxide**
Senko TMCTS	1.7×10^{-4}	4.2×10^{-4}
DIC PMP	1.8×10^{-4}	2.1×10^{-4}
CMS 7	2.3×10^{-3}	4.3×10^{-3}
HC Target Values	$>7\times10^{-5}$	$>8\times10^{-4}$

eter for the specific gas. Ideally, given the approximate nature of the estimated K_m targets above, appropriate composite hollow fiber membranes for the Hattler Catheter should incorporate a design safety factor and possess membrane permeances 2 to 3 times larger than given above. Not surprisingly, considering our previous estimate of composite fiber membrane permeance associated with a "normal" permeability nonporous polymer, the identification and/or development of a suitable composite hollow fiber for the Hattler Catheter, along with associated studies of membrane permeance, have been central components of our catheter development effort.

Despite its central importance, not much information exists on membrane permeances for composite hollow fiber membranes suitable for the Hattler Catheter. Kamo et al.[56] measured the O_2 membrane permeance for the Mitsubishi Rayon MHF series of composite hollow fibers and reported K_m values from 0.9×10^{-6} to 1.6×10^{-6} ml/(cm^2•s•cm Hg), significantly below the membrane permeance target for the Hattler Catheter. Although the MHF composite fibers would not be suitable for the Hattler Catheter and would significantly affect overall gas exchange, the relatively small K_m of the MHF series is not surprising given the "normal" permeability (~ 1 Barrier) of polyurethane used for the nonporous polymer layer. Our laboratory has conducted its own extensive studies of membrane permeance of candidate composite hollow fibers for the Hattler Catheter, using a gas-liquid measurement system described previously along with a simpler gas-gas measurement system.[57,58] Candidate composite hollow fibers include 1) Senko TMCTS Coated Fiber (Senko Medical Instruments Manufacturing Company, Japan), a Celgard x30-240 microporous fiber coated with a plasma polymerized layer of tetramethylcyclotetrasiloxane (TMCTS); 2) DIC PMP Fiber (Dainippon Ink and Chemical, Japan), an asymmetric fiber constructed from a microporous poly-4-methyl-pentene-1 (PMP) with sealed outer pores (see Figure 6.12); and 3) CMS 7 Fiber (Compact Membrane Systems, Wilmington, DE), a proprietary coating of a Teflon copolymer on a Celgard x30-240 fiber. Table 6.3 compares membrane permeance values determined from gas-gas measurements on these composite hollow fibers[57] with the target membrane permeances for the Hattler Catheter. All candidate composite fibers achieve suitable K_m for O_2, but the target K_m value for CO_2 is more difficult to achieve and becomes the limiting constraint. The membrane permeance of the Senko fiber for CO_2 is about half the K_m target, which suggests that the Senko fiber in the Hattler Catheter could effect a 10%-20% reduction in overall CO_2 gas exchange. The only composite hollow fiber satisfying both the O_2 and CO_2 targets for membrane permeance is the CMS fiber, with K_m values at least 4 times the targets. Ultimately, the selection of a suitable composite hollow fiber for the Hattler Catheter will not only consider membrane gas permeance, but will also weigh manufacturing issues, biocompatibility (both natural biocompatibility and the suitability for surface modification of the fiber, e.g., with heparin attachment), and long term stability.

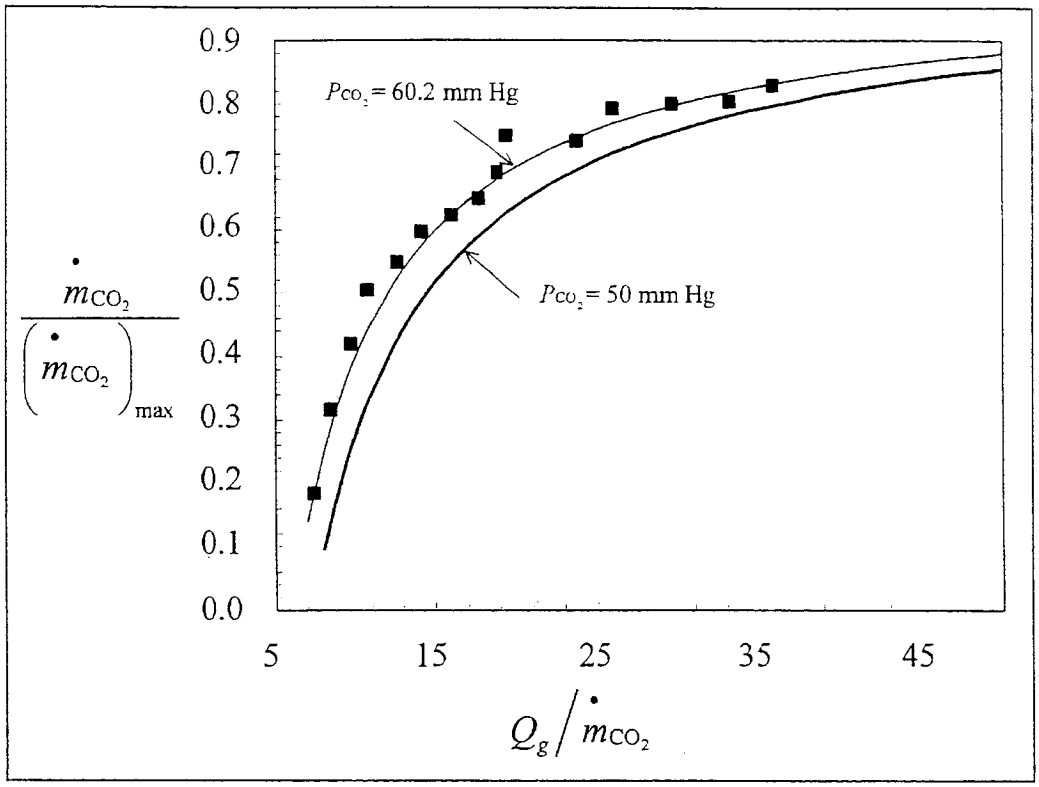

Fig. 6.13. Effect of sweep gas flow rate on carbon dioxide exchange. Solid lines based on predictions from simple model and symbols are experimental data on an extracorporeal blood oxygenator.

Role of Gas-Side Flow and Pressure

Gas flow through the Hattler Catheter does not directly affect the overall gas permeance, K, of the device because, as discussed previously, the overall permeance is dictated principally by liquid-side gas permeance, conditioned by diffusional boundary layers at the fiber surfaces, and secondarily by membrane permeance. Nevertheless, the dynamics of sweep gas flow through the Hattler Catheter do affect overall gas exchange by a direct effect on gas-side partial pressures of O_2 and CO_2, and by the resulting impact on the partial pressure driving force for exchange of these gases (see Eq. 6.1). The rate of gas flow through the Hattler Catheter principally affects the CO_2 exchange rate, while the pressure drop across the fiber bundle arising from the gas flow principally affects the O_2 exchange rate.

The dependence of CO_2 exchange on gas flow rate arises because the partial pressure of CO_2 in blood available for driving exchange is relatively low, approximately 40 to 60 mm Hg, and hence even a small buildup in CO_2 within the sweep gas pathway can markedly diminish the PCO_2 gradient between blood and gas flowing through the device. Thus, a direct relation exists between the actual rate of CO_2 exchange, the gas flow rate through the device, and the degree to which insufficient gas flow may be reducing CO_2 exchange. We previously developed a simple model describing the interrelationship between gas flow rate and CO_2 exchange rate in an artificial lung like the Hattler Catheter.[60] The model uses appropriate normalization to arrive at a universal relation between gas flow rate and CO_2 exchange that is independent of device specific mass transfer features of the artificial

lung, e.g., the overall device permeance K. The effect of sweep gas flow rate, Q_g, on CO_2 exchange, $(\dot{m}_{co_2})_{max}$, is given by:

$$\frac{\dot{m}_{co_2}}{\left(\dot{m}_{co_2}\right)_{max}} = 1 - \frac{P_{g,o}}{2(\overline{P_{co_2}})_b} \frac{1}{\left(\frac{Q_g}{\dot{m}_{co_2}}\right)}, \qquad \text{(Eqn. 6.10)}$$

where $(\dot{m}_{co_2})_{max}$ is the maximum possible rate of CO_2 exchange in the limit of infinite gas flow, $P_{g,o}$ is the outlet pressure of the sweep gas, and $(\overline{P_{co_2}})_b$ is the mean blood side partial pressure of CO_2 within the fiber bundle.[61] This simple theoretical relation, shown graphically in Figure 6.13, helps delineate regimes between relatively gas flow dependent and gas flow independent CO_2 exchange. At a $(\overline{P_{co_2}})_b$ of 50 mm Hg, the CO_2 exchange rate is within 15% of the maximum attainable exchange when $\left(\frac{Q_g}{\dot{m}_{co_2}}\right) > 50$, which has become a useful criterion for specifying required gas flow rates of the Hattler Catheter. For example, if a CO_2 exchange rate of 125 ml/min is a nominal target value for a specific Hattler Catheter, then the gas pathways of the device need to be designed for sweep gas flows exceeding 50 x 125 ml/min or 6.3 l/min. Otherwise, the reduction in CO_2 exchange by insufficient gas flow will be appreciable. The theoretical prediction of the effect of gas flow rate on CO_2 exchange (i.e., Eq. 6.10) was recently validated experimentally for standard extracorporeal blood oxygenators.[61] As indicated in Figure 6.13, the experimental relation between CO_2 exchange and gas flow rate (squares) agreed well with the theoretical predictions based on the $(\overline{P_{co_2}})_b$ of 60.2 mm Hg measured during the CO_2 exchange experiment.

In the same gas flow rate range where CO_2 exchange is dependent on gas flow rate, the O_2 exchange rate is essentially independent of gas flow rate per se. This is so because the buildup in CO_2 within the sweep gas, although significant from the perspective of the gradient in PCO_2 between blood and gas phase, has a much smaller impact on the gradient in PO_2 between blood and gas phase. In this gas flow rate range (essentially the one shown in Figure 6.13), the sweep gas remains more than 95% O_2. Hence, the principal determinant of the partial pressure of O_2 in the gas-phase, and the PO_2 gradient between blood and gas, is the average total gas pressure in the fibers. Thus, although gas flow rate does not directly affect O_2 exchange, it does so indirectly because of the pressure drop engendered by the gas flow through the fiber bundle. The Hattler Catheter operates at subatmospheric (vacuum) pressures and has been designed with a negligible inlet sweep gas pressure drop, so that the sweep gas enters the fiber bundle at approximately atmospheric pressure. Accordingly, the average gas-side partial pressure of O_2 in the Hattler Catheter (vacuum-driven gas flow), $(\overline{Po_2})_g$ can be approximated by:

$$(\overline{P_{co_2}})_g \cong P_{atm} - \frac{(\Delta P)_g}{2}, \qquad \text{(Eqn. 6.11)}$$

where $(\Delta P)_g$ is the gas-side (intrafiber) pressure drop, which is dependent on gas flow rate, fiber lumen size and number of fibers within the bundle. The fiber bundle pressure drop can be predicted accurately based on compressible Poiseuille flow theory through parallel tubes.[62]

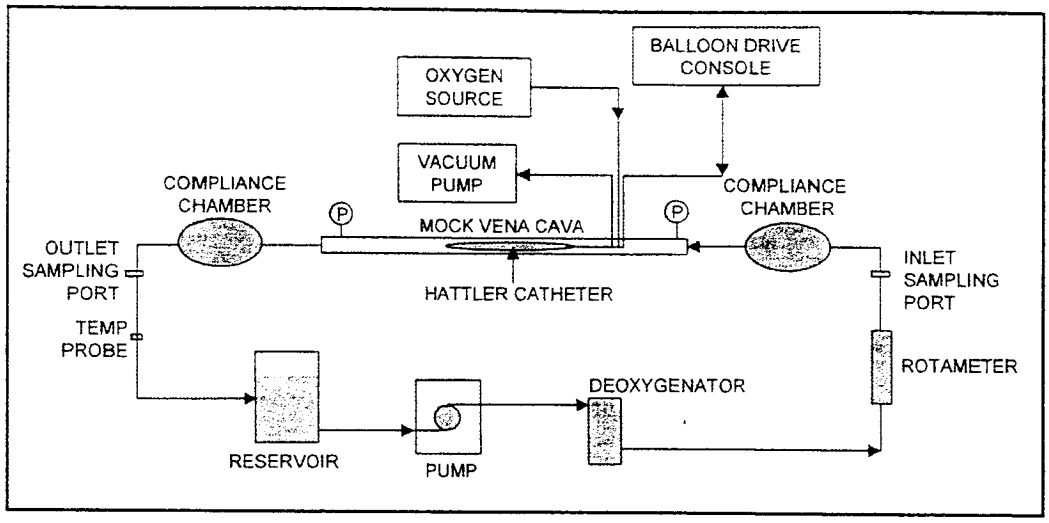

Fig. 6.14. Mock vena cava (MVC) flow loop used for bench testing of gas exchange in the Hattler Catheter.

Hattler Catheter Development

Constraints associated with insertion and vena cava placement place limits on the fiber surface area of an intravascular artificial lung like the Hattler Catheter. Thus, the gas exchange efficiency (gas exchange per unit surface area) of the Hattler Catheter must exceed that of standard extracorporeal blood oxygenators, which can increase membrane area to accomplish a desired level of gas exchange. Our nominal design goal for gas exchange in the Hattler Catheter is 125 ml/min with a 0.5 m^2 device, which represents a gas exchange efficiency of 250 ml/min•m^2, over twice that of typical extracorporeal blood oxygenators. The Hattler Catheter uses balloon pulsation as a simple approach to improve its gas exchange efficiency for O_2 and CO_2 exchange. Balloon pulsation drives *additional* convective blood flow, beyond that which would otherwise exist in the vena cava, across the hollow fibers in a mainly cross-flow fashion to the fibers, as opposed to the mostly parallel flow that normal vena cava blood flow would impart. As described above, the altered flow pattern and the increase in convective flow velocity past the fibers reduces the diffusional boundary layers on the fiber surfaces, thus increasing the liquid-side gas permeance K_l and improving gas transfer efficiency.

The development work towards improving balloon pulsation and gas exchange in the Hattler Catheter made extensive use of a simple and repeatable bench test of gas exchange, the experimental setup of which is as shown in Figure 6.14. The bench test setup consists principally of a mock vena cava (MVC: a one inch internal diameter Plexiglas or Tygon tube) within which the Hattler Catheter is placed, a pump for providing steady controlled flow rate through the MVC, a deoxygenator for establishing appropriate levels of inlet gas tension to the MVC, compliance chambers for accommodating balloon pulsation, and pre and post MVC sampling ports. A Hattler Catheter under test is placed within the MVC and perfused with distilled water at 3 l/min and 37° C. Pure O_2 sweep gas is run through the Hattler Catheter under vacuum at 3 l/min, and the O_2 and CO_2 exchange rates, $\dot{m}_{o_2}$ and $\dot{m}_{co_2}$, are determined over a full range of balloon pulsation rates. The O_2 exchange rate is computed from the product of the Po_2 difference in water across the test section (determined from samples at the pre and post MVC ports), water flow rate, and the solubility of O_2 in the water, while the CO_2 exchange is computed from the product of

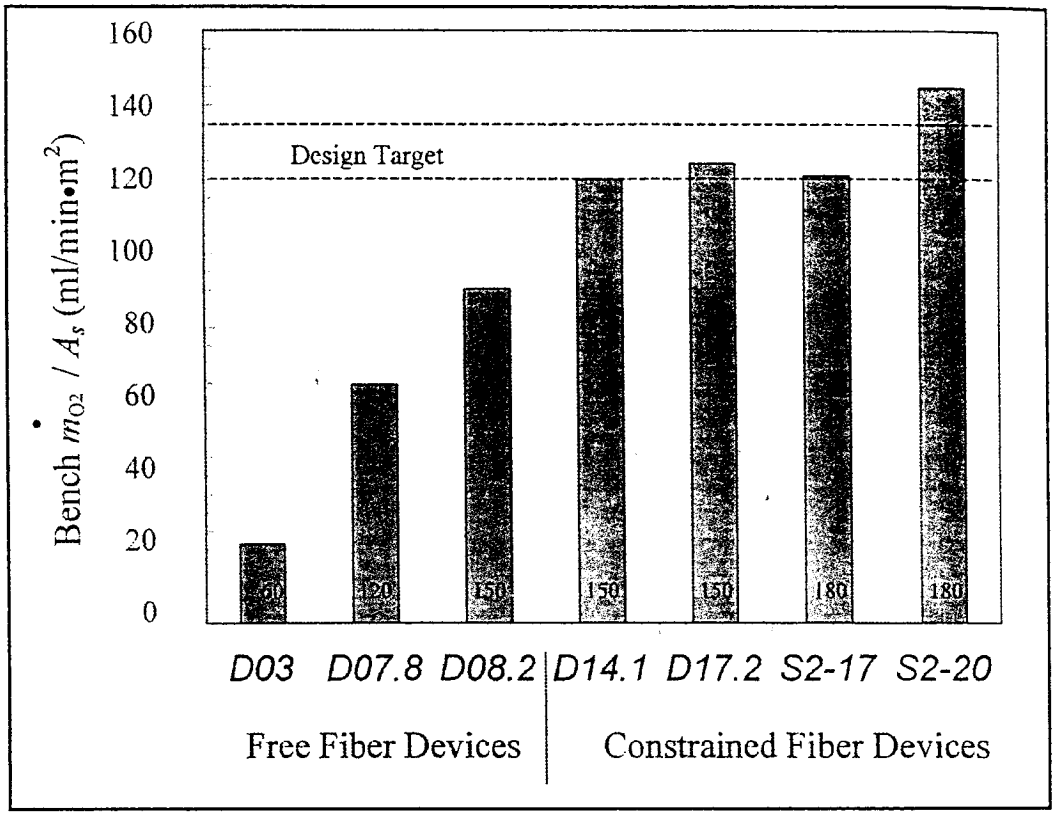

Fig. 6.15. Improvements in oxygen exchange associated with development of the Hattler Catheter, as measured in the MVC bench test using water at 3 l/min. Principal improvements came from greater achievable balloon pulsation rates (beats per minute, bpm, for each device shown within data bars) and use of fiber bundles made from fiber fabric (constrained fiber devices) rather than free fiber.

gas flow rate and the gas-side CO_2 fraction leaving the device. The bench tests use water rather than blood as the test fluid to simplify testing and to facilitate multiple experiments on a given Hattler Catheter device. The CO_2 and O_2 exchange rates in water are less than would occur in blood due to effective solubility differences. Indeed, the O_2 exchange in water is several-fold smaller than in blood because of the marked increase in effective solubility provided by hemoglobin. A mathematical model has been developed for O_2 exchange in the Hattler Catheter to help relate gas exchange performance in water to that in blood.[63,64] For physiologically relevant conditions of flow and inlet , the model analysis suggests that O_2 exchange rates in blood are 2-3 fold greater than those in water. Thus, our design goal for gas exchange efficiency of 250 ml/min•m^2 conservatively becomes a target of 125 ml/min•m^2 for O_2 exchange in our water bench test in the MVC.

The recent development history of the Hattler Catheter, from the perspective of the maximum O_2 exchange rate achieved by select devices in the MVC bench test, is summarized in Figure 6.15. Significant improvements in gas exchange occurred as optimization of the gas flow paths in the Hattler Catheter allowed for balloon pulsation at larger frequencies. Each of the devices shown had 40 ml balloons. The maximum pulsation frequency for each device is given within their respective data bars. The ability to effectively pulsate the balloon of a Hattler Catheter is studied with the device placed within a sealed-chamber plethysmograph, in which the swings in chamber pressure transduce balloon volume changes. In this manner, dynamic volume excursions of the balloon can be

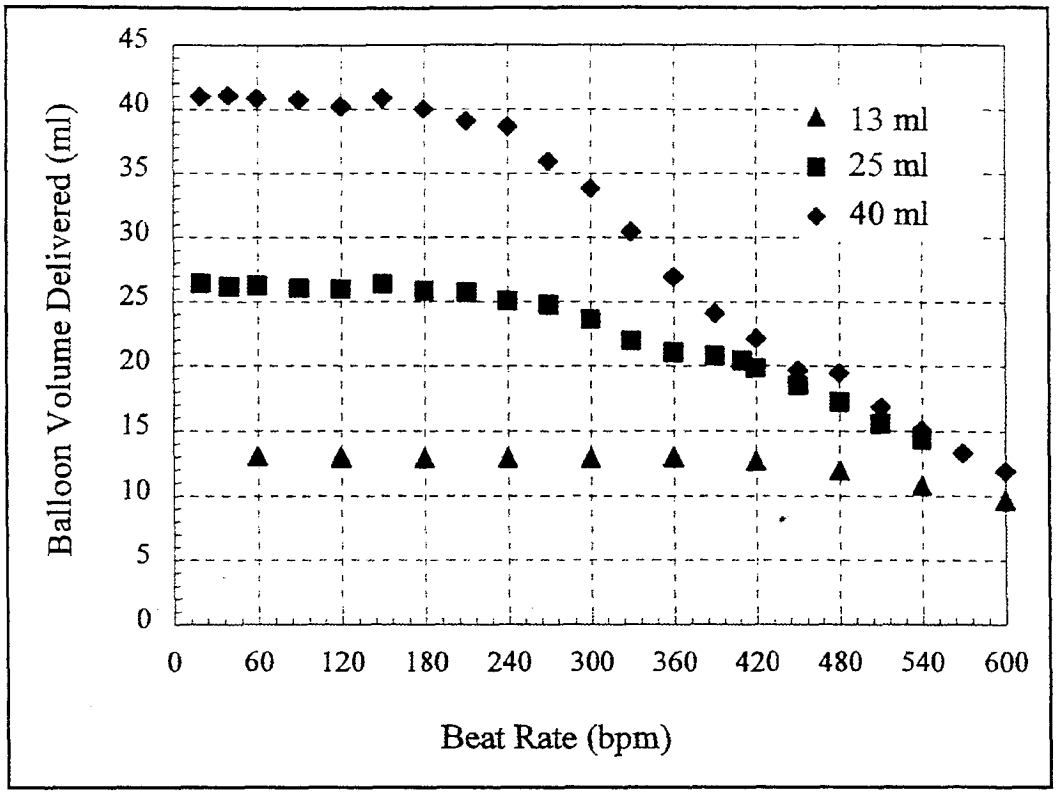

Fig. 6.16. Dynamic balloon volume swings measured for Hattler Catheters with 13 ml, 25 ml and 40 ml balloons using pneumatic balloon drive system. Effective balloon pulsation, with complete filling and emptying of balloon can be achieved approximately up to 500 bpm for the smallest ballon (13 ml), 300 bpm for the intermediate-sized balloon (25 ml) and 200 bpm for the largest balloon (40 ml).

accurately determined over a broad range of pulsation frequencies. Early Hattler Catheter devices could only pulsate effectively, with full filling and emptying of the 40 ml balloon, up to 50-60 beats per minute (bpm), as evidenced by the D03 device in Figure 6.15. Our current gas pathway design for the Hattler Catheter allows a 40 ml balloon to pulsate effectively up to 180 bpm, as seen for the S2 devices in Figure 6.15. The actual dynamic balloon volumes measured using the balloon plethysmograph for several recent Hattler Catheter devices with 40 ml, 25 ml, and 13 ml balloons are shown in Figure 6.16 as a function of pulsation rate. Frequencies of 180 to 200 bpm can be consistently reached for Hattler Catheters with 40 ml balloons and frequencies of 300-400 bpm can be reached for Hattler Catheters with 10-25 ml balloons.

Another significant improvement in gas exchange for the Hattler Catheter occurred with use of constrained fiber bundles made from fiber fabrics, rather than free fiber bundles (Fig. 6.15).[65] Constrained fiber bundles help keep fibers fixed so as to increase the relative velocity of blood flow past the fibers by not allowing fiber movement by the blood. Moreover, the fiber fabrics enforce a more uniform spacing between fibers (see Fig. 6.17). As a result, the fibers are kept more evenly distributed around the pulsating balloon, thereby increasing the uniformity of balloon generated blood flow through the fiber bundle. The increase in blood flow velocity past the fibers, occurring more uniformly throughout the fiber bundle, reduces the average size of the diffusional boundary layers on the fiber surfaces and increases the liquid-side gas permeance of the Hattler Catheter. Bench tests of gas exchange for Hattler Catheter devices with a free fiber bundle and a constrained fiber

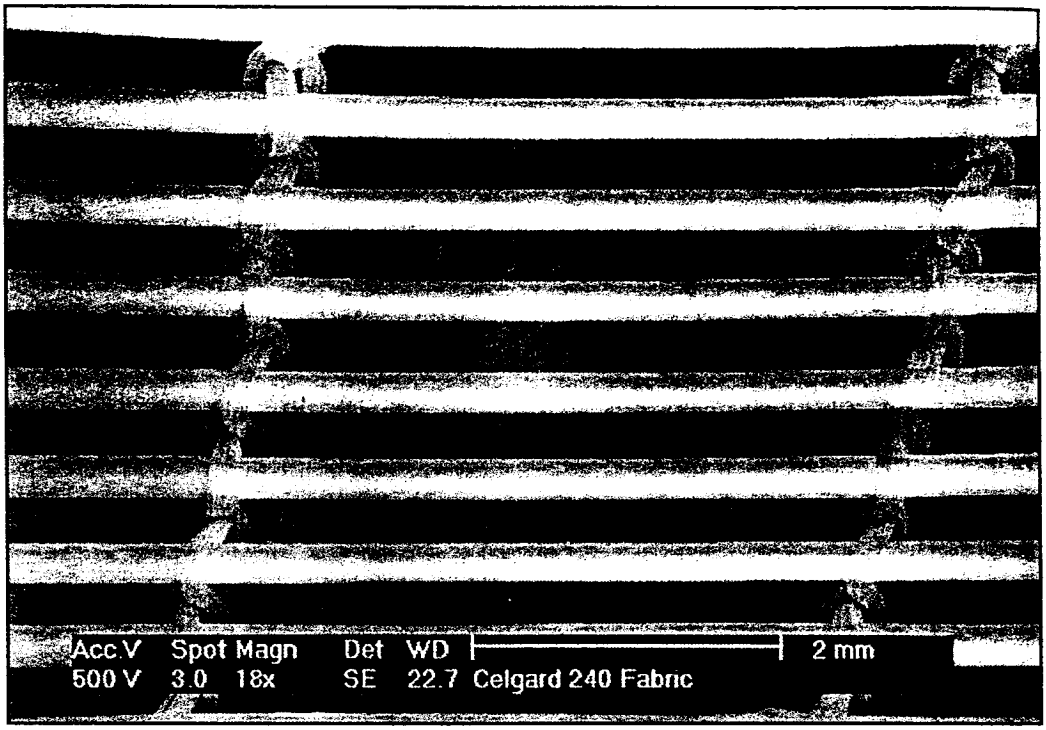

Fig. 6.17. Fiber fabric used to make the fiber bundle for the Hattler Catheter. The fabric uses Celgard x30-240 hollow fiber membranes knit using support threads into a uniform spaced fiber array.

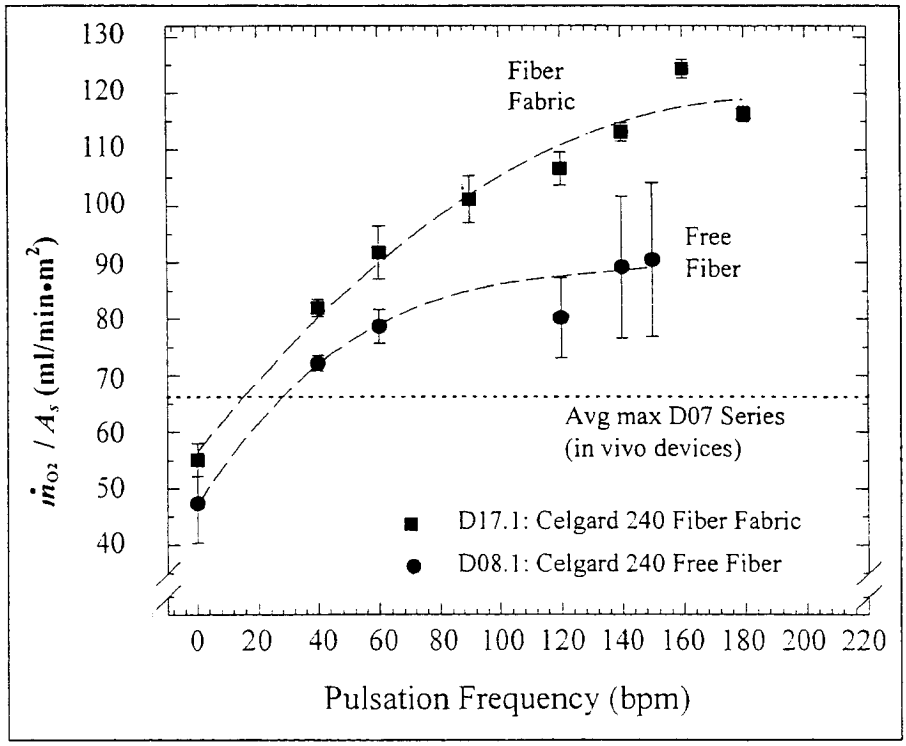

Fig. 6.18. Oxygen exchange as a function of balloon pulsation rate for otherwise comparable Hattler Catheters made using fiber fabric (constrained fiber device) versus free fiber. Data from bench test in MVC using water at 3 l/min.

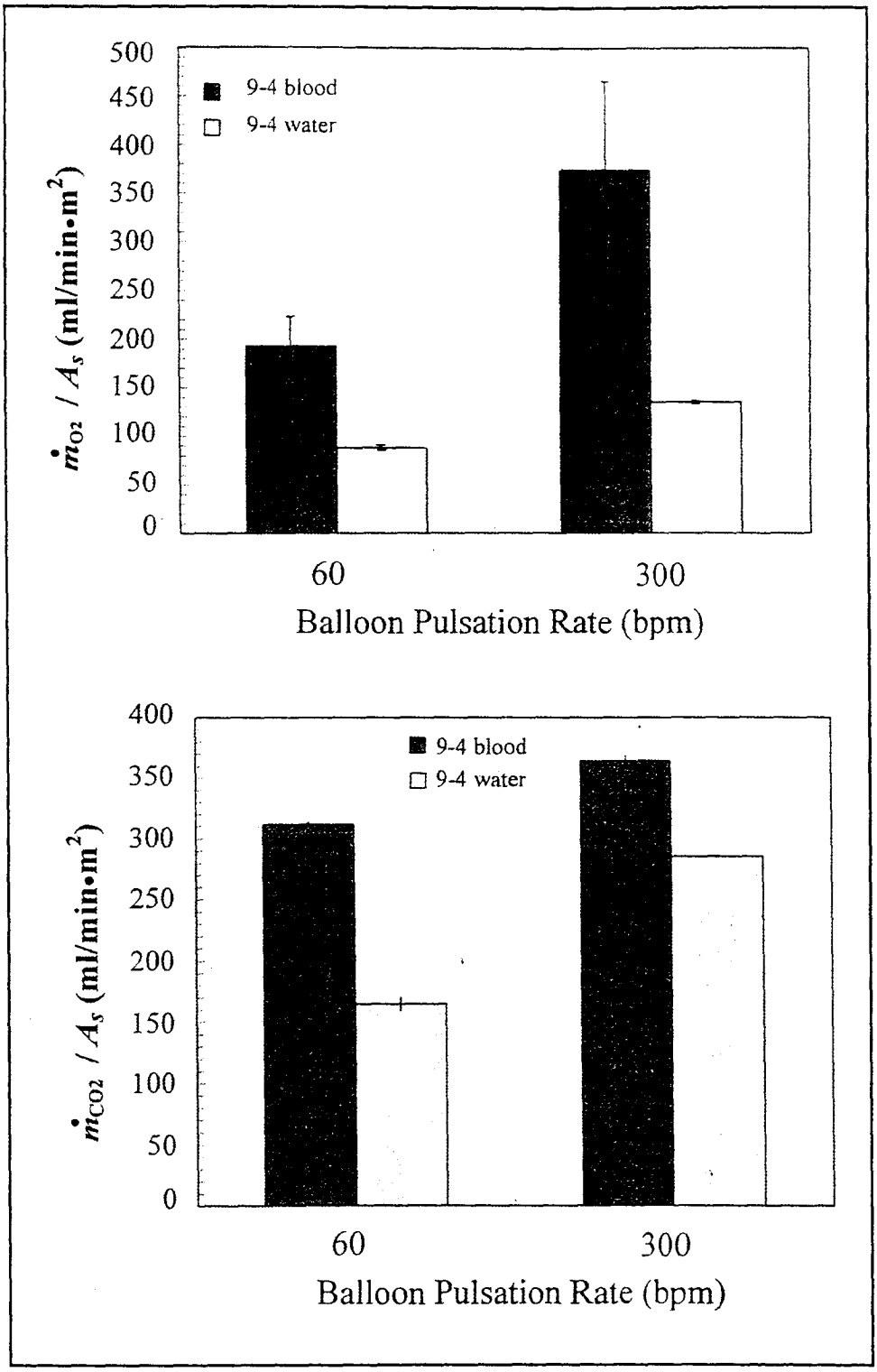

Fig. 6.19. Oxygen exchange (top panel) and carbon dioxide exchange (bottom panel) for the same Hattler Catheter device perfused with blood versus water in the MVC bench test.

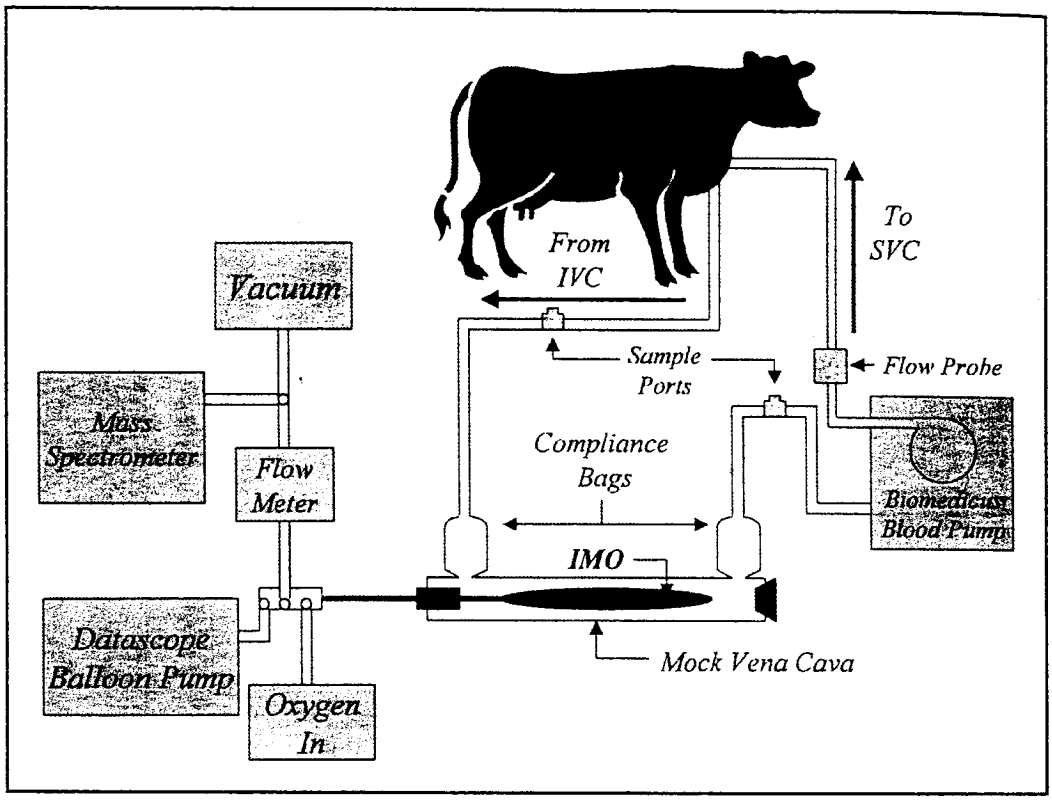

Fig. 6.20. Mock vena cava flow loop used for ex vivo animal tests.

bundle, but otherwise identical, showed that the free fiber device tended to plateau in oxygen exchange with increasing balloon pulsation rate, while the constrained fiber device did not (Fig. 6.18). Furthermore, gas exchange for the free fiber Hattler Catheter exhibited more variability associated with device position and orientation within the mock vena cava (MVC) test section. The combined effect of balloon pulsation at higher rates and more effective exploitation of balloon pulsation using constrained fiber bundles have resulted in Hattler Catheters which have reached the targeted level of O_2 exchange in our water bench tests, as can be seen in the development summary graph (Fig. 6.15).

The bench tests of gas exchange in the Hattler Catheter can also be done using the same MVC setup but using prepared bovine blood and AAMI blood test conditions.[52] The bench tests in blood help establish a benchmark for the gas exchange levels that might be achieved during animal implantation, and also help further establish the correspondence between bench tests in water versus the same tests in blood. Since blood tests are more intensive and difficult, they are reserved for select Hattler Catheter designs, while all Hattler Catheters within and across design series undergo the water bench test for gas exchange. The gas exchange levels achieved during bench tests in water and blood are compared for the same Hattler Catheter device in Figure 6.19. Gas transfer efficiency for O_2 and CO_2 reached 360 and 350 ml/min•m^2, respectively, in blood under maximal pulsation conditions (300 bpm for these devices, which had 25 ml balloons). These same pulsation conditions yielded O_2 and CO_2 exchange rates of 120 and 280 ml/min•m^2 for O_2 and CO_2, respectively, in water. Overall, these bench tests of the Hattler Catheter in blood help confirm that current devices produce gas exchange levels at or above our design target. Accordingly, recent efforts have focused more intensely on establishing the performance of

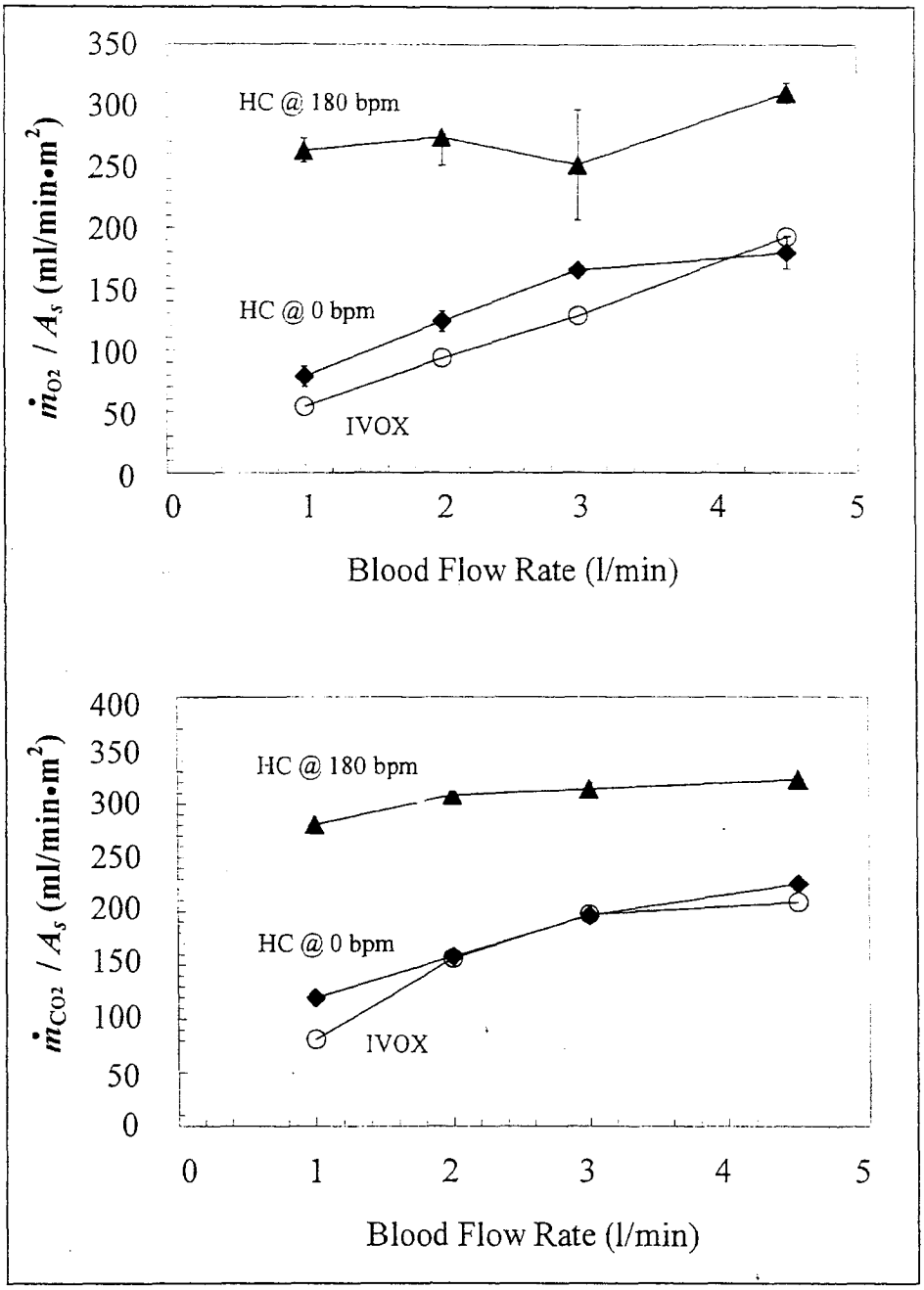

Fig. 6.21. Oxygen exchange (top panel) and carbon dioxide exchange (bottom panel) for the Hattler Catheter in the ex vivo animal tests. Gas exchange is shown for the Hattler Catheter without balloon pulsation and with maximal balloon pulsation at 180 bpm. Also shown for comparison is the reported gas exchange achieved by the IVOX in a similar ex vivo animal test using sheep.[69] All gas exchange values normalized to device surface area.

the Hattler Catheter in animal tests, and on using the animal test plan to further define and refine the Hattler Catheter design for ultimate human implantation.

Animal Tests of the Hattler Catheter

The Hattler Catheter has been tested in calves (of approximately 70-90 kg weight) using ex vivo (extracorporeal) circuit tests and in vivo implantations, both acute and chronic.

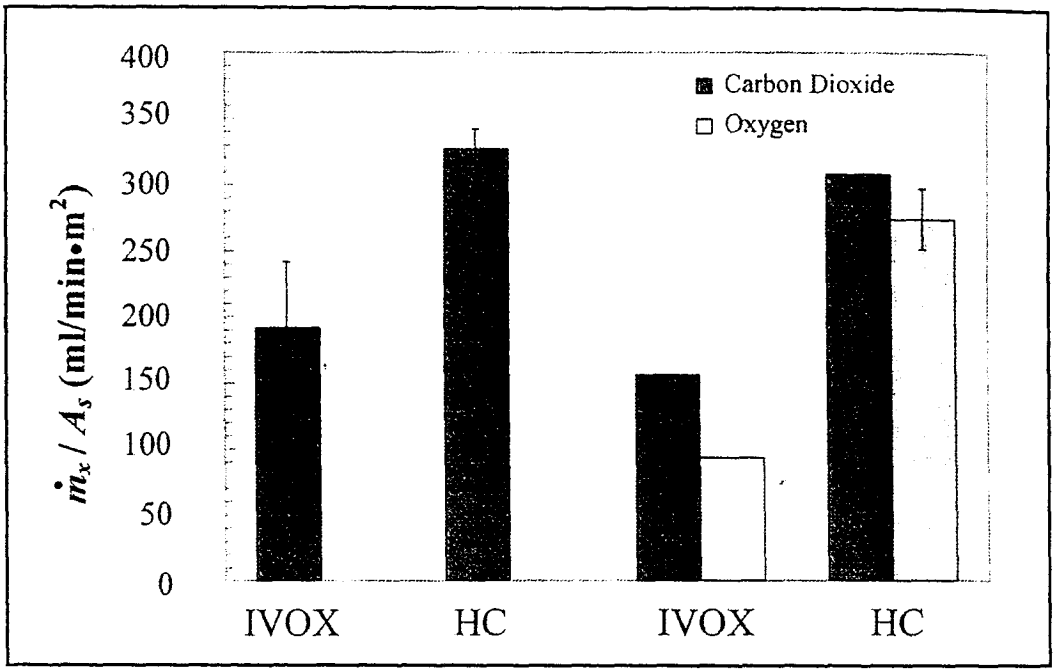

Fig. 6.22. Carbon dioxide exchange for the Hattler Catheter determined during acute animal implantation (average and standard deviation shown for N=4 calves). Also shown for comparison are reported data for IVOX in sheep implantation[70] and a summary of ex vivo O_2 and CO_2 exchange at 2 l/min blood flow for the Hattler Catheter and the IVOX from previous figure.

The ex vivo circuit tests involve placing the Hattler Catheter within a mock vena cava (as used in the bench test setup) that is attached to a bypass-like blood circuit.[66] While the extracorporeal tests allow for the tight control, monitoring and variation of key covariates, including the blood flow rate past the catheter, they do not mimic the implantation setting within the vena cava. In the vena cava the Hattler Catheter must accommodate to the venous anatomy and to venous blood flow patterns, where numerous venous tributaries adjacent to the device increase blood exposure to the fiber bundle even without balloon pulsation. Moreover, blood flow past the Hattler Catheter within the vena cava may be conditioned by or be dependent on the flow resistance offered by the device. Finally, ex vivo experiments are, by necessity, short term (5-8 hours) and cannot be used to evaluate the response of the biological and physiological systems of the animal to the device, either acutely or chronically, in which case the calves are allowed to awaken, stand up and otherwise function normally.

The ex vivo circuit test in the mock vena cava is an important evaluative assessment of gas exchange for the Hattler Catheter.[66] The circuit consists of a mock vena cava or MVC (a 1 inch Tygon tube) and compliance bags connected to a blood circuit that is perfused off an anesthetized calf using a Biomedicus blood pump, as shown in Figure 6.20. The circuit perfuses the MVC with fresh bovine blood at controlled flow rates and is otherwise similar to the bench test setup (Fig. 6.14), but without the deoxygenator and heat exchanger. Blood is drawn by a drainage catheter passed into the inferior vena cava from the right atrium and returned through a separate catheter positioned in the upper superior vena cava from an insertion site at the jugular vein. The ex vivo test enables evaluation of the gas exchange performance of the Hattler Catheter under conditions of known flow and vessel geometry. More importantly, the ex vivo test is comparable to that used previously to evaluate the clinically utilized IVOX device. Thus, direct comparisons can be made

under controlled conditions between the gas exchange performance of the Hattler Catheter and the IVOX device.

The O_2 exchange rate measured in the ex vivo test of the Hattler Catheter is compared to that for the IVOX device in Figure 6.21. The comparisons are done over a physiologically relevant range of blood flow rates through the mock vena cava. Gas exchange results for the Hattler Catheter are shown both without and with maximal balloon pulsation (180 bpm for the HC device tested in this study). Across the blood flow rate range studied, the maximum O_2 exchange rate of the Hattler Catheter varied from 250 to 310 ml/min•m^2, which is consistent with projections based on bench characterization tests of gas exchange in water, although slightly less than achieved during actual bench tests using blood (Fig. 6.19). Overall, oxygen exchange for the Hattler Catheter in the ex vivo test was 2-4 times greater than that reported for the IVOX in comparable ex vivo testing. Similar results were found for the CO_2 exchange rate of the Hattler Catheter, and the comparisons with the IVOX during ex vivo testing are shown in Figure 6.21. Across the blood flow rate range studied, the CO_2 exchange rate of the Hattler Catheter varied from 280 to 340 ml/min•m^2 and was 1.5 to 3 times greater than that for the IVOX device. In both the O_2 and CO_2 exchange performance, balloon pulsation appears to have a significant effect on the dependence of gas exchange on blood flow rate. Whereas the IVOX shows variability in gas exchange with blood flow rate, as does the Hattler Catheter with no balloon pulsation (0 bpm), balloon pulsation in the Hattler Catheter at 180 bpm eliminates much if not all dependence of gas exchange on blood flow rate. An important potential implication of this result is that with variations in vena caval blood flow rate within and among patients (e.g., due to differences in cardiac output), the Hattler Catheter may show more consistent gas exchange levels clinically than did the IVOX device.

Implantation of the Hattler Catheter in calves provides another important evaluative test of device performance and is a key test of device interaction with a real biological/physiological system.[67] In the implantation tests, the calves are instrumented so that arterial, pulmonary, central venous, and inferior vena caval pressures can be simultaneously recorded and those sites used for blood sampling. A Swan-Ganz thermal dilution catheter is connected to a cardiac output monitor. The calf is heparinized and the device inserted with a surgical cut-down into the jugular vein and positioned within the inferior vena cava, right atrium, and terminal superior vena cava. While O_2 exchange rates are difficult to determine during implantation tests, the CO_2 exchange rate can be reliably determined by measuring the gas flow rate and CO_2 fraction of the exhaust gas leaving the Hattler Catheter. We recently completed a series of acute implants of the Hattler Catheter in four calves, with the devices placed within the right atrium and inferior vena cava.[67] As shown in Figure 6.22, the maximum CO_2 exchange rate (normalized to the device surface area) averaged 327 ± 15 ml/min•m^2 over the series of calf implants. Moreover, the CO_2 transfer rate was over 70% greater than reported for the clinically tested IVOX implanted acutely in sheep. The calf and sheep are analogous models for CO_2 exchange, hence, the difference in CO_2 exchange rate reflects differences in the gas exchange performance of the Hattler Catheter compared to the IVOX. The gas exchange levels accomplished by the Hattler Catheter during implantation are also consistent with those from the ex vivo tests (shown for comparison in Figure 6.22), as is the improvement compared to the IVOX. The CO_2 exchange rate shown in Figure 6.22 is for our current Hattler Catheter design with constrained fiber bundles and is significantly greater than the CO_2 exchange rate we reported of 140 to 180 ml/min•m^2 based on an earlier implantation study using a previous Hattler Catheter design (D07 series) with free fiber bundles and reduced balloon pulsatility.[68] The

Table 6.4. Effect of permissive hypercapnia on carbon dioxide exchange**

Venous P_{CO_2} (mm Hg)	$\dot{m}_{co_2}$ normalized to $\dot{m}_{co_2}$ at 49.1 mm Hg	P_{CO_2}/49.1
49.1 (baseline)	1	1
54.3	1.13	1.11
60.2	1.33	1.23
63.3	1.44	1.29
66.9	1.48	1.36

** Hattler Catheter device 10-7 during acute implantation in calf.

improvement in in vivo gas exchange attributable to constrained fiber bundles and improved balloon pulsation in the Hattler Catheter is approximately twofold and is generally consistent with the improvement seen during bench tests of these devices (see Fig. 6.15).

The CO_2 exchange rate of the Hattler Catheter can also be increased naturally by use of permissive hypercapnia, in which venous levels of P_{CO_2} are allowed to increase above normal. As the venous level of P_{CO_2} rises, so does the gradient for CO_2 diffusion from blood to sweep gas, thus increasing the CO_2 exchange rate within the Hattler Catheter according to Equation 6.1 (written for CO_2). Table 6.4 shows the increase in CO_2 exchange rate measured during permissive hypercapnia from a baseline venous P_{CO_2} of 49 mm Hg to an elevated P_{CO_2} of 67 mm Hg during implantation of the Hattler Catheter in a calf. The CO_2 exchange rate is shown as the fractional increase relative to that at the baseline P_{CO_2}. The Hattler Catheter increased its CO_2 exchange rate by 48% in response to the permissive hypercapnia, an increase somewhat greater than the percent increase in P_{CO_2} associated with the hypercapnia. Thus, permissive hypercapnia represents a promising strategy for further augmenting CO_2 removal with the Hattler Catheter.

Implantation of the Hattler Catheter in calves does not engender significant changes in cardiac output nor in other measured hemodynamic or hematological parameters. In our recent series of acute implantations of the Hattler Catheter,[67] the decrease in cardiac output with insertion relative to baseline (preinsertion) was less than 10-15% for devices with 25 ml balloons (N=4), although larger changes were seen when implanting devices with larger diameter, 40 ml balloons (unpublished observation). Plasma-free hemoglobin rose no higher than 10-15 mg% after 6-8 hours of acute implantation and platelet count dropped an average of 30% in the early phase of implantation (0-2 hours) but stabilized thereafter. In our chronic experiments (N=7), plasma-free hemoglobin peaked at an average high of 11.5 ± 4.9 mg%, but by the end of the experiment (2-3 days) dropped to an average of 4.9 ±3.6 mg% (unpublished observation).

The Hattler Catheter has progressed from basic bench research through small and large animal studies to a point where it is now ready for human implantation. Although the application of the technology in the research setting has evolved over the last 16 years, the basic bioengineering principles upon which it is founded have not changed and have allowed progress to a point where 50% of basal requirements for O_2 and CO_2 exchange in man can be met in a manner that is both dependable and reproducible. There is reason to anticipate, therefore, that direct intravenous gas exchange as a new approach for the support of the acutely injured lung will be a reality in the near future.

Acknowledgements

1. The work described in this chapter from our group was supported by the U.S. Army Medical Research, Development, Acquisition and Logisitcs command under prior Contract No. DAMD17-94-C-4052 and current Grant No. DAMD17-98-1-8638. The views, opinions and/or findings contained in this report are those of the authors and should not be construed as an Official Department of the Army position, policy or decision unless so designated by other documentation.
2. The authors wish to thank the research staff and students of the Artificial Lung Laboratory: Joseph Golob, Brian Frankowski, Thomas Merrill, Laura Lund, Heide Russian, Michael Lann, Tamara Tulou, Mariah Hout and Monica Garcia. We also appreciate the assistance of Ms. Alison Bushey in preparing the final manuscript.

References

1. Ashbaugh DG, Bigelow DB, Petty TL et al. Acute respiratory distress in adults. Lancet 1967; 2:319-323.
2. Zilberberg MD, Epstein SK. Acute lung injury in the medical ICU: Comorbid conditions, age, etiology, and hospital outcome. Am J Respir Crit Care Med 1998; 157:1159-1164.
3. Bernard GR, Artigas A, Brigham KL et al. The American-European Consensus Conference on ARDS: Definition, mechanisms, relevant outcomes, and clinical trial coordination. Am J Respir Crit Care Med 1994; 149:818-824.
4. Doyle RL, Szaflarski N, Modin GW et al. Identification of patients with acute lung injury: Predictors of mortality. Am J Respir Crit Care Med 1995; 152:1818-1824.
5. Luhr OR, Antonsen K, Karlsson M et al. Incidence and mortality after acute respiratory failure and acute respiratory distress syndrome in Sweden, Denmark, and Iceland. Am J Respir Crit Care Med 1999; 159:1849-1961.
6. Linde-Zwirble WT, Clermont G, Coleman MB et al. Incidence of ARDS in the US, Europe, and Japan. Intensive Care Med 1996; 22 (Suppl. 3):272.
7. Angus DC, Linde-Zwirble WT, Clermont G et al. What's the incidence and mortality of ARDS in the US? Am J Respir Crit Care Med 1996; 153;4:A592.
8. University Health System Consortium. Oak Brook, Illinois, 1996.
9. The Acute Respiratory Distress Syndrome Network. Ventilation with lower tidal volumes as compared with traditional tidal volumes for acute lung injury and the acute respiratory distress syndrome. N Engl J Med 2000; 342:1301-1308.
10. Hirschl RB, Pranikoff T, Wise C et al. Initial experience with partial liquid ventilation in adult patients with the acute respiratory distress syndrome. JAMA 1996; 275:383-389.
11. Fort P, Farmer C, Westerman J et al. High-frequency oscillatory ventilation for adult respiratory distress syndrome—Pilot study. Crit Care Med 1997; 25:937-947.
12. Anzueto A, Baughman RP, Guntupalli KK et al. Aerosolized surfactant in adults with sepsis-induced acute respiratory distress syndrome. N Eng J Med 1996; 334: 1417-1421.
13. Dellinger RP, Zimmerman JL, Taylor RW et al. Effects of inhaled nitric oxide in patients with acute respiratory distress syndrome: Results of a randomized phase II trial. Crit Care Med 1998; 26:15-23.
14. The Acute Respiratory Distress Syndrome Network. Ketoconazole does not reduce mortality in patients with the acute respiratory distress syndrome. JAMA 2000; 283:1995-2002.
15. Federspiel W, Sawzik P, Borovetz H et al. Temporary support of the lungs: the artificial lung. In: Cooper DKC, Miller LW, Patterson GA., eds. Transplantation and Replacement of Thoracic Organs. 2nd ed. Dudrecht: Kluwer Academic Publishers, 1996:717-728.
16. Hattler BG, Johnson PC, Sawzik PJ et al. Respiratory dialysis: A new concept in pulmonary support. ASAIO J 1992; 38:M322-M325.
17. Reeder GD, Hattler BG, Rawleigh J et al. Current progress in the development of an intravenous membrane oxygenator. ASAIO J 1993; 39:M461-M465.
18. Hattler BG, Reeder GD, Sawzik PJ et al. Development of an intravenous membrane oxygenator (IMO): Enhanced intravenous gas exchange through convective mixing of blood around hollow fiber membranes. Artif Organs 1994; 18:806-812.

19. Hattler BG, Reeder GD, Sawzik, PJ et al. Development of an intravenous membrane oxygenator: A new concept in mechanical support for the failing lung. J Heart and Lung Trans 1995; 13:1003-1007.
20. Federspiel WJ, Hewitt T, Hout MS et al. Recent progress in engineering the Pittsburgh intravenous membrane oxygenator. ASAIO J 1996; 42:M435-M442.
21. Macha M, Federspiel WJ, Lund LW et al. Acute in vivo studies of the Pittsburgh intravenous membrane oxygenator. ASAIO J 1996; 42:M609-M615.
22. Mortensen JD. An intravenacaval blood gas exchange (IVCBGE) device: A preliminary report. Trans Am Soc Artif Intern Org 1987; 33:570-573.
23. Gattinoni L, Kolobow T, Tomlinson T et al. Low frequency positive pressure ventilation with extracorporeal carbon dioxide removal (LFPPV-ECCO$_2$R): An experimental study. Anesth Analg 1978; 57:470-476.
24. Hickling KG, Walsh J, Henderson S et al. Low mortality rate in adult respiratory distress syndrome using low-volume, pressure-limited ventilation with permissive hypercapnia: A prospective study. Crit Care Med 1994; 22:1568-1578.
25. Hickling KG, Henderson SJ, Jackson R. Low mortality associated with low volume pressure limited ventilation with permissive hypercapnia in severe adult respiratory distress syndrome. Intensive Care Med 1990; 16:372-377.
26. Weinberger SE, Schwartzstein RM, Weiss JW. Hypercapnia. N Engl J Med 1989; 321:1223-1227.
27. Stewart TE, Meade MO, Cook DJ et al. Evaluation of a ventilation strategy to prevent barotrauma in patients at high risk of acute respiratory distress syndrome. N Engl J Med 1998; 338:355-361.
28. Brochard L, Roudot-Thoraval F, Roupie E et al. Tidal volume reduction for prevention of ventilator-induced lung injury in acute respiratory distress syndrome. Am J Respir Crit Care Med 1998; 158:1831-1838.
29. Brower RG, Shanholtz CB, Fessler HE et al. Prospective, randomized, controlled clinical trial comparing traditional versus reduced tidal volume ventilation in acute respiratory distress syndrome patients. Crit Care Med 1999; 27:1492-1498.
30. Ware LB, Matthay MA. .The acute respiratory distress syndrome. N Engl J Med 2000; 342:1334-1349.
31. Slutsky AS, Tremblay LN. Multiple system organ failure: Is mechanical ventilation a contributing factor? Am J Respir Crit Care Med 1998; 157:1721-1725.
32. Ranieri VM, Suter PM, Tortorella C et al. Effect of mechanical ventilation on inflammatory mediators in patients with acute respiratory distress syndrome: a randomized controlled trial. JAMA 1999; 282:54-61.
33. Slutsky AS. Lung injury caused by mechanical ventilation. Chest 1999; 116:9S-15S.
34. Tremblay L, Valenza F, Riberio SP et al. Injurious ventilation strategies increase cytokines and c-fos m-RNA expression in an isolated rat lung model. J Clin Invest 1997; 99:944-952.
35. Pugin J, Verghese G, Widmer MC et al. The alveolar space is the site of intense inflammatory and profibrotic reactions in the early phase of acute respiratory distress syndrome. Crit Care Med 1999; 27:304-312.
36. Pugin J, Ricou B, Steinberg KP et al. Proinflammatory activity in bronchoalveolar lavage fluids from patients with ARDS, a prominent role for interleukin-1. Am J Respir Crit Care Med 1996; 153:1850-1856.
37. Pinsky MR. Heart-lung interactions. In: Marini JJ, Slutsky AS, eds. Physiological Basis of Ventilatory Support. New York: Marcel Dekker, 1998; 491-531.
38. Borelli M, Fumagalli R, Bernasconi F et al. Relief of hypoxemia contributes to a reduction in cardiac index related to the use of positive end-expiratory pressure. Intensive Care Med 1996; 22:382-386.
39. Fagon JY, Chastre J, Domont Y et al. Nosocomial pneumonia in patients receiving continuous mechanical ventilation. Am Rev Respir Dis 1989; 139:877-884.
40. Zapol WM, Snider MT, Hill JD et al. Extracorporeal membrane oxygenation in severe acute respiratory failure: a randomized prospective study. JAMA 1979; 242:2193-2196.
41. Gattinoni L, Pesenti A, Mascheroni D et al. Low-frequency positive pressure ventilation with extracorporeal CO_2 removal in severe acute respiratory failure. JAMA 1986; 256:881-886.
42. Morris AH, Wallace CJ, Menlove RL et al. Randomized clinical trial of pressure controlled inverse ratio ventilation and extracorporeal CO_2 removal for adult respiratory distress syndrome. Am J Respir Crit Care Med 1994; 149:295-305.

43. Brunel F, Belgheth M, Mira J et al. Extracorporeal carbon dioxide removal and low-frequency positive-pressure ventilation: improvement in arterial oxygenation with reduction of risk of pulmonary barotrauma in patients with adult respiratory distress syndrome. Chest 1993; 104:889-898.
44. Manert W, Haller M, Briegel J et al. Venovenous extracorporeal membrane oxygenation (ECMO) with a heparin-lock bypass system: An effective addition in the treatment of acute respiratory failure (ARDS). Anesthetist 1996; 45:438-448.
45. Kolla S, Awad SS, Rich PB et al. Extracorporeal life support for 100 adult patients with severe respiratory failure. Ann Surg 1997; 226:544-566.
46. Goodman LR. Congestive heart failure and adult respiratory distress syndrome: New insights using computed tomography. Radiol Clin North Am 1996; 34:33-46.
47. Gattinoni L, Bombino M, Pelosi P et al. Lung structure and function in different stages of severe adult respiratory distress syndrome. JAMA 1994; 271:1772-1779.
48. Muller EE, Kolobow T, Mandava S et al. How to ventilate lungs as small as 12.5% of normal: The new technique of intratracheal pulmonary ventilation. Ped Res 1993; 34:606-610.
49. Mortensen JD. Intravascular oxygenator: A new alternative method for augmenting blood gas transfer in patients with acute respiratory failure. Artif Org 1992; 16:75-82.
50. Conrad SA, Bagley A, Bagley B et al. Major findings from the clinical trials of the intravascular oxygenator. Artif Org 1994; 18:846-863.
51. Konishi R, Shimizer R, Firestone L et al. Nitric oxide prevents human platelet adhesion to fiber membranes in whole blood. ASAIO J 1996; 42:M850-M853.
52. AAMI Standards and Recommended Practices. Association for the Advancement of Medical Instrumentation. Volume 2.1 Biomedical Equipment, Part 1, Equipment Therapy and Surgery. Cardiovascular implants and artificial organs: blood gas exchangers. AAMI 1996; 7199:633-648.
53. Montoya JP, Shanley CJ, Merz SI et al. Plasma leakage through microporous membranes: Role of phospholipids. ASAIO J 1992; 38:M399-M405.
54. Mottaghy K, Oedekoven B, Starmans H et al. Technical aspects of plasma leakage prevention in microporous capillary membrane oxygenators. ASAIO J 1989; 35:640-643.
55. Brodkey RS, Hershey HC. Transport Phenomena: A Unified Approach. New York: McGraw-Hill Book Company, 1988:182-186.
56. Kamo J, Uchida M, Hirai T et al. A new multilayered composite hollow fiber membrane for artificial lung. Artif Org 1990; 14:369-372.
57. Lund LW. Measurement of Hollow Fiber Membrane permeance in a Gas-Liquid System. Ph.D. Thesis. University of Pittsburgh, 2000.
58. Lund LW, Federspiel WJ, Hattler BG. Gas permeability of hollow fiber membranes in a gas-liquid system. J Membr Sci 1996; 117:207-219.
59. Lund LW, Hattler BG, Federspiel WJ. Is condensation the cause of plasma leakage in microporous hollow fiber membrane oxygenators? J Membr Sci 1998; 147:87-93.
60. Federspiel WJ, Hattler BG. Sweep gas flowrate and CO_2 exchange in artificial lungs. Artif Org 1996; 20:1050-1056.
61. Hout MS, Hattler BG, Federspiel WJ. Validation of a model for flow-dependent carbon dioxide exchange in artificial lungs. Artif Org 2000; 24:114-119.
62. Federspiel WJ, Williams JL, Hattler BG. Gas flow dynamics in hollow fiber membranes. AIChE 1996; 42:2094-2099.
63. Hewitt TJ, Hattler BG, Federspiel WJ. A mathematical model of gas exchange in an intravenous membrane oxygenator. Ann Biomed Eng 1998; 26:166-178.
64. Federspiel WJ, Hewitt TJ, Hattler BG. Experimental evaluation of a model for oxygenation exchange in a pulsating intravascular artificial lung. Ann Biomed Eng 2000; 28:160-167.
65. Federspiel WJ, Hout MS, Hewitt TJ et al. Development of a low flow resistance intravenous oxygenator. ASAIO J 1997; 45:M725-M730.
66. Federspiel WJ, Golob JF, Merrill TL et al. Ex-vivo testing of the intravenous membrane oxygenator (IMO). ASAIO J 2000; 46:261-267.
67. Golob JF, Federspiel WJ, Merrill TL et al. Acute in-vivo testing of an intravascular oxygenator. ASAIO J. In press.
68. Macha M, Federspiel WJ, Lund L et al. Acute in-vivo studies of the Pittsburgh intravenous membrane oxygenator. ASAIO J 1996; 42:M609-M615.
69. Tao W, Zwischenberger JB, Nguyen TT et al. Performance of an intravenous gas exchanger (IVOX) in a venovenous bypass circuit. Ann Thorac Surg 1994; 57:1484-1490.

70. Zwischenberger JB, Cox CS Jr, Graves D et al. Intravascular membrane oxygenation and carbon dioxide removal—A new application for permissive hypercapnia? Thorac Cardiovasc Surg 1992; 40:115-120.